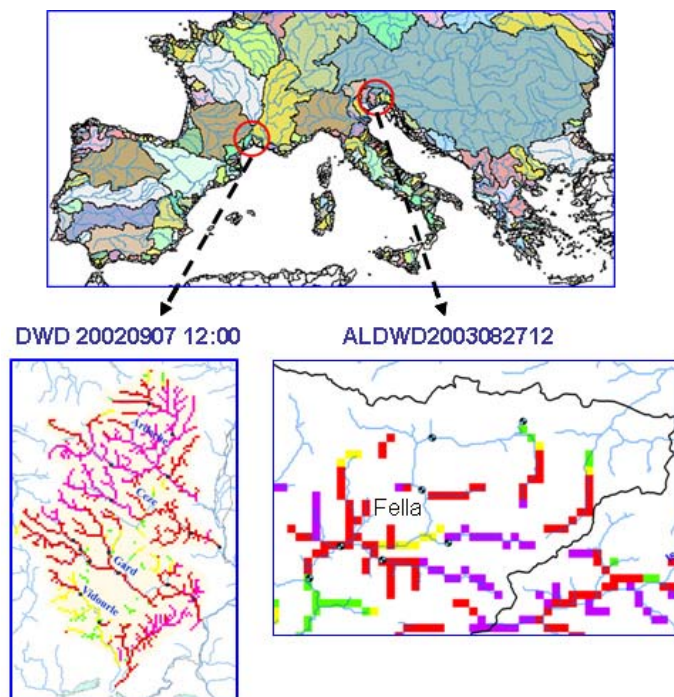




## Early Flash Flood Warning:

A feasibility study with a distributed hydrological model and threshold exceedance

Jalal Younis & Jutta Thielen





## **Early Flash Flood Warning:**

**A feasibility study with a distributed hydrological model and  
threshold exceedance**

The mission of the Institute for Environment and Sustainability is to provide scientific-technical support to the European Union's Policies for the protection and sustainable development of the European and global environment.

European Commission  
Joint Research Centre  
Institute for Environment and Sustainability

**Contact information**

Address: TP 261  
E-mail: [jalal.younis@jrc.it](mailto:jalal.younis@jrc.it), [jutta.thielen@jrc.it](mailto:jutta.thielen@jrc.it)  
Tel.: +39 0332 78 5455  
Fax: +39 0332 78 6653

<http://ies.jrc.ec.europa.eu/>  
<http://www.jrc.ec.europa.eu/>

**Legal Notice**

Neither the European Commission nor any person acting on behalf of the Commission is responsible for the use which might be made of this publication.

***Europe Direct is a service to help you find answers  
to your questions about the European Union***

**Freephone number (\*):  
00 800 6 7 8 9 10 11**

(\* Certain mobile telephone operators do not allow access to 00 800 numbers or these calls may be billed.

A great deal of additional information on the European Union is available on the Internet. It can be accessed through the Europa server <http://europa.eu/>

JRC 48916

EUR 23637 EN  
ISSN 1018-5593  
ISBN: 978-92-79-09689-1  
DOI: 10.2788/38120  
Luxembourg: Office for Official Publications of the European Communities

© European Communities, 2008

Reproduction is authorised provided the source is acknowledged

*Printed in Italy*



## **Abstract**

*In Mediterranean Europe, flash flooding is one of the most devastating hazards in terms of loss of human life and infrastructures. Over the last two decades, flash floods have caused damage costing a billion Euros in France alone. One of the problems of flash floods is that warning times are very short, leaving typically only a few hours for civil protection services to act. This study investigates if operationally available short-range numerical weather forecasts together with a rainfall-runoff model can be used for early indication of the occurrence of flash floods.*

*One of the challenges in flash flood forecasting is that the watersheds are typically small, and good observational networks of both rainfall and discharge are rare. Therefore, hydrological models are difficult to calibrate and the simulated river discharges cannot always be compared with ground measurements. The lack of observations in most flash flood prone basins, therefore, necessitates the development of a method where the excess of the simulated discharge above a critical threshold can provide the forecaster with an indication of potential flood hazard in the area, with lead times of the order of weather forecasts.*

*This report is focused on four case studies in Mediterranean part of Europe: i) The September 2002-flash flood event in the Cévennes-Vivarais region in the Southeast of the Massif Central in France, a region known for devastating flash flood; ii) the August 2003-flash flood event in both Fella subcatchment of Tagliamento watershed and upstream part of Isonzo river basin, iii) the October 2006-flash flood event in Isonzo river basin and iv) the September 2007-flash flood event in Upper Sava river basin in Slovenia. The French case study is described in more detail with the principles and methodologies being explained that are then applied to the remaining three case studies. Also, there were more data available for the 1<sup>st</sup> case study.*

*The critical aspects of using numerical weather forecasting for flash flood forecasting are being described together with the threshold – exceedance approach previously postulated for the European Flood Alert System (EFAS). The short-range weather forecasts, from the Local model of the German national weather service, are driving the LISFLOOD model, a hybrid between conceptual and physically based rainfall-runoff model. Results of the study indicate that high resolution operational weather forecasting combined with a rainfall-runoff model could be useful to determine flash floods more than 24 hours in advance.*



## Table of contents

1. Introduction .....	2
2. Hydrological model, input data and methodologies.....	4
2.1. The hydrological LISFLOOD model .....	4
2.2. Mathematical Formulations of the hydrological processes in LISFLOOD .....	5
2.3. Input data.....	8
2.4. Methodology of discharge threshold exceedances.....	9
3. Case studies .....	11
3.1. The flash flood event 8-9th September 2002 – France.....	11
3.1.1. The Cévennes - Vivarais region in Southern France.....	11
3.1.2. Description of the 8-9th September 2002 case study.....	14
3.1.3. Input data for the study .....	15
3.1.4. Hydrological regime and calculation of thresholds .....	16
3.1.5. Forecasting the 8-9th September 2002 event .....	21
3.1.6. Assessments of hits, false alarms and missed events over a 6 months forecasting period.....	26
3.2. Flash flood event 29th August 2003 in river basins in Italy and Slovenia.....	32
3.2.1. The Fella River Basin of Eastern Italian Alps.....	32
3.2.2. The Soca (Isonzo) River Basin .....	35
3.2.3. Description of the 29th August 2003 case study .....	36
3.2.4. Input data for the two studies .....	40
3.2.5. Results.....	41
3.3. The flash flood event 24th October 2006 – Slovenia .....	44
3.3.1. The Goriska Region North-West part of Slovenia.....	44
3.3.2. Description of the 24th October 2006 case study.....	45
3.3.3. Results.....	47
4. Summary and Conclusions.....	50
References.....	52

# 1. Introduction

Flash floods are rapidly developing floods with devastating effects for the environment and high risk of loss of life. In Mediterranean Europe, flash flooding is classified as one of the most devastating hazards in terms of human life loss and infrastructures (Gruntfest and Handmer, 1999). Over the last two decades, flash floods caused a billion Euros of damage in France alone (Hauet et al., 2003, in French). Apart from the economic impact, flash floods are life threatening: 11 victims were reported in the Nîmes event (1988), 58 during the Vaison la Romaine flash flood (1992) (Senesi et al., 1996), 35 for the Aude storms (1999) (Ducrocq et al., 2003) and 24 for the 2002 Gard event (Delrieu et al., 2005; Hauet et al., 2003) which is presented here. Vulnerability to flash floods will probably increase in the coming decades due to evolving land use and the modification of the pluviometric regime associated with the evolution of the climate (Parry, et al., 2007, Palmer and Raisanen, 2002, Rosso and Rulli, 2002).

A flash flood is typically the consequence of a short-duration storm event. The term “flash” refers to the rapid response, with water levels in the drainage network reaching a crest within minutes to a few hours after the onset of the rain event, leaving extremely short time for warning. Flash flood generating storms can accumulate more than 200mm during less than 6 hours over natural watersheds ranging in area from 25 to 2500 km<sup>2</sup> (Creutin and Borga, 2003; Collier, 2007). Over built-up areas of 1 to 100 km<sup>2</sup>, flash floods can be produced by storms of even shorter duration with accumulations of over 50mm in less than one hour (Creutin and Borga, 2003; Collier, 2007). The rising rate of waters of several m.h<sup>-1</sup> and the flow velocity of several m.s<sup>-1</sup> make these floods far more dangerous for human lives than large river floods (excluding dam breaks). Furthermore, the danger also comes from the rarity of the phenomenon which imposes a new observation strategy as well as new forecasting methodology.

One of the greatest difficulties in addressing flash flood problems is defining them (Montz and Gruntfest, 2002) and the conditions playing roles in flash flooding are their sudden occurrence with short lead time for warning, fast-moving and generally violent, jeopardizing life, damaging properties and infrastructure. They are also distinguished by their small spatial scales (generally less than 1000 km<sup>2</sup>) of drainage basins in which flooding occur. Aside from intense rainfall and small net storm motion, factors that contribute strongly to flash flooding are low permeability or saturated soils, impervious ground surfaces, and steep slopes. Failure of small to medium-sized dams, including debris dams, contributes significantly to the fatalities and damage associated with flash floods. A majority of flash-flood-related deaths occur in motor vehicles as people seek shelter and/or try to escape from rising waters.

The meteorological conditions leading to flash floods are mostly severe convective systems that typically develop under potentially unstable conditions released by localized trigger mechanisms. Due to their very localized nature, the observation of these events with a gauging network is problematic. Weather radars can provide better spatial rainfall estimations. However, it has been demonstrated that the more intense the rainfall, the less reliable the rainfall estimates from radar become (Austin, 1987, BASC, 2005, Borga et al., 2002, Ciach et al., 2000,). Therefore accurate monitoring and prediction of severe storm rainfall intensities continue to be a major challenge. Prediction of these events with numerical meteorological models is even more difficult (Fritsch et al., 1998; Anquetin et al., 2005; Chancibault et al., 2006; Yates et al., 2007) due to the strong interaction of different physical and micro-physical processes across different scales.

One accepted method for predicting flash floods in ungauged river basins is so called “flash flood guidance” (Georgakakos, 2006). Flash flood guidance is a general term referring to the average rain needed over an area and during a specific time necessary to initiate rapid flooding in small streams. Depending on the method also the antecedent soil moisture or precipitation from previous days is taken into account.

However, there is no unique and simple theory about the runoff production on watersheds during flood events. The main reason is that a variety of processes can be involved which are usually grouped in two categories: saturation excess (Dunne process) or infiltration excess (Horton runoff). Due to the high heterogeneity and space variability of the watershed characteristics (land use, soil type and depth, subsoil, local slope, upstream contributing area) and to antecedent moisture conditioning, these processes are likely to be active at the same time in various combinations.

Therefore, in order to forecast flash-floods reliably, the temporal and spatial resolved scales of the meteorological and hydrological model should be linked. Recognition of the need to couple meteorological and hydrological processes in interpretative studies and in the development of predictive models for flash floods has been demonstrated (Anquetin et al., 2004).

In this study a regional approach for flash flood warning also in ungauged river basins is being proposed. The concept is based on the principle of discharge threshold exceedances as opposed to a rainfall exceedance (Georgakakos, 2006). A discharge threshold exceedance approach is currently being explored for river flood forecasting (Thielen et al., 2008, Ramos et al., 2007), but has also been recently applied for flash floods, for instance by Reed et al. (2007).

In section 3 three case studies were chosen for regions lying within the Mediterranean climate zone, the Cévennes - Vivarais region in Southern France, the Friuli region of Eastern Italian Alps with its neighboring Isonzo watershed in Slovenia and the Goriska and Gorenjska Regions North-West part of.

## 2. Hydrological model, input data and methodologies

### 2.1. The hydrological LISFLOOD model

LISFLOOD is a GIS-based hydrological rainfall-runoff-routing model that is capable of simulating the hydrological processes that occur in a catchment. The specific development objective was to produce a tool that can be used in large and trans-national catchments for a variety of applications, including flood forecasting, and assessing the effects of river regulation measures, land-use change and climate change. Although a wide variety of existing hydrological models are available that are suitable for each of these individual tasks, few single models are capable of doing all these jobs. Besides this, our objective requires a model that is spatially distributed and –at least to a certain extent- physically-based (van der Knijff, Younis and de Roo, 2008). A brief model description is given below, more detail can be found in the LISFLOOD manual (van der Knijff and de Roo, 2008).

Figure 2.1.1 gives an overview of the structure of the LISFLOOD model. Basically, the model is made up of the following components:

- a 2-layer soil water balance sub-model
- sub-models for the simulation of groundwater and subsurface flow (using 2 parallel interconnected quasi-linear reservoirs)
- a sub-model for the routing of surface runoff to the nearest river channel
- a sub-model for the routing of channel flow (not shown in the Figure)

The processes that are simulated by the model include snow melt (not shown in the Figure), infiltration, interception of rainfall, leaf drainage, evaporation and water uptake by vegetation, surface runoff, preferential flow (bypass of soil layer), exchange of soil moisture between the two soil layers and drainage to the groundwater, sub-surface and groundwater flow, and flow through river channels. Upward vertical soil moisture and groundwater flow (capillary rise) are not simulated, and neither are deep groundwater systems. This poses some limitations on the use of LISFLOOD in areas that are either very dry or have a hydrology that is heavily influenced by deep groundwater, or combinations of both. (van der Knijff, Younis and de Roo, 2008).

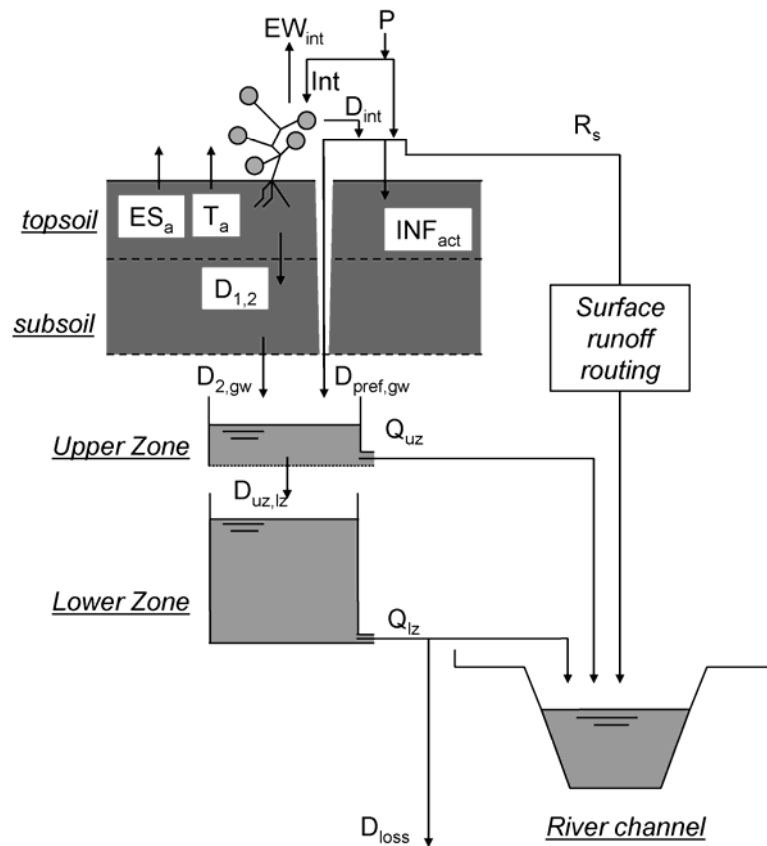


Fig 2.1.1: Overview of the LISFLOOD model. P = precipitation; Int = interception; EW<sub>int</sub> = evaporation of intercepted water; D<sub>int</sub> = leaf drainage; ES<sub>a</sub> = evaporation from soil surface; T<sub>a</sub> = transpiration (water uptake by plant roots); INF<sub>act</sub> = infiltration; R<sub>s</sub> = surface runoff; D<sub>1,2</sub> = drainage from top- to subsoil; D<sub>2,gw</sub> = drainage from subsoil to upper groundwater zone; D<sub>pref,gw</sub> = preferential flow to upper groundwater zone; D<sub>uz,lz</sub> = drainage from upper- to lower groundwater zone; Q<sub>uz</sub> = outflow from upper groundwater zone; Q<sub>lz</sub> = outflow from lower groundwater zone; D<sub>loss</sub> = loss from lower groundwater zone. Note that snowmelt is not included in the Figure (even though it is simulated by the model) (van derKnijff et al., 2008).

## 2.2. Mathematical Formulations of the hydrological processes in LISFLOOD

### Rain and snow

If the average temperature is below 1°C, all precipitation is assumed to be snow. A snow correction factor is used to correct for undercatch of snow precipitation. Unlike rain, snow accumulates on the soil surface until it melts. The rate of snowmelt is estimated using a simple degree-day factor method. Degree-day factor type snow melt models usually take the following form (e.g. see WMO, 1986):

$$M = C_m(T_{avg} - T_m) \quad (2-1)$$

where  $M$  is the rate of snowmelt,  $T_{avg}$  is the average daily temperature,  $T_m$  is some critical temperature and  $C_m$  is a degree-day factor [ $\text{mm } ^\circ\text{C}^{-1} \text{ day}^{-1}$ ]. Speers et al. (1979) developed an extension of this equation which accounts for accelerated snowmelt that takes place when it is raining (cited in Young, 1985):

$$M = (0.074 + 0.007 \cdot R)(T_{avg} - T_m) \quad (2-2)$$

where  $R$  is the daily rainfall and both  $M$  and  $R$  are expressed in cm (rather than mm). The equation is supposed to apply when rainfall is greater than 3 cm in 24 hours. Moreover, although the equation is reported to work sufficiently well in forested areas, it is not valid in areas that are above the tree line, where radiation is the main energy source for snowmelt). Currently LISFLOOD uses a variation on the equation of Speers et al. The modified equation simply assumes that for each mm of rainfall, the rate of snowmelt increases with 1% (compared to a 'dry' situation). This yields the following equation:

$$M = C_m(1 + 0.01 \cdot R\Delta t)(T_{avg} - T_m) \cdot \Delta t \quad (2-3)$$

where  $M$  is the snowmelt per time step [mm],  $R$  is rainfall (not snow!) intensity [ $\text{mm day}^{-1}$ ], and  $\Delta t$  is the time interval [days].  $T_m$  has a value of  $0^\circ\text{C}$ , and  $C_m$  is set to a default value of  $4.5 \text{ mm } ^\circ\text{C}^{-1} \text{ day}^{-1}$ . However, it should be stressed that the value of  $C_m$  can actually vary greatly both in space and time (e.g. see Martinec et al., 1998). Therefore, in practice this parameter is often treated as a calibration constant. The amount of snowmelt can never exceed the actual snow cover that is present on the surface.

### **Frost index soil**

When the soil surface is frozen, this affects the hydrological processes occurring near the soil surface. To estimate whether the soil surface is frozen or not, a frost index  $F$  is calculated. The equation is based on Molnau & Bissell (1983, cited in Maidment 1993), and adjusted for variable time steps. The rate at which the frost index changes is given by:

$$\frac{dF}{dt} = -(1 - A_f)F - T_{av} \cdot e^{-0.04 \cdot K \cdot d_s / we_s} \quad (2-4)$$

$dF/dt$  is expressed in [ $^\circ\text{C day}^{-1} \text{ day}^{-1}$ ].  $A_f$  is a decay coefficient [ $\text{day}^{-1}$ ],  $K$  is a snow depth reduction coefficient [ $\text{cm}^{-1}$ ],  $d_s$  is the (pixel-average) depth of the snow cover (expressed as mm equivalent water depth), and  $we_s$  is a parameter called snow water equivalent, which is the equivalent water depth water of a snow cover (Maidment, 1993). In LISFLOOD,  $A_f$  and  $K$  are set to 0.97 and  $0.57 \text{ cm}^{-1}$  respectively, and  $we_s$  is taken as 0.1, assuming an average snow density of  $100 \text{ kg/m}^3$  (Maidment, 1993). The soil is considered frozen when the frost index rises above a critical threshold of 56. For each time step the value of  $F$  [ $^\circ\text{C day}^{-1}$ ] is updated as:

$$F(t) = F(t-1) + \frac{dF}{dt} \Delta t \quad (2-5)$$



$F$  is not allowed to become less than 0.

### **Interception**

Interception is estimated using the following storage-based equation (Aston, 1978, Merriam, 1960):

$$Int = S_{max} \cdot [1 - \exp(-k \cdot R\Delta t / S_{max})] \quad (2-6)$$

where  $Int$  [mm] is the interception per time step,  $S_{max}$  [mm] is the maximum interception,  $R$  is the rainfall intensity [mm day<sup>-1</sup>] and the factor  $k$  accounts for the density of the vegetation.  $S_{max}$  is calculated using an empirical equation (Von Hoyningen-Huene, 1981):

$$\begin{cases} S_{max} = 0.935 + 0.498 \cdot LAI - 0.00575 \cdot LAI^2 & [LAI > 0.1] \\ S_{max} = 0 & [LAI \leq 0.1] \end{cases} \quad (2-7)$$

where  $LAI$  is the average Leaf Area Index [m<sup>2</sup> m<sup>-2</sup>] of each model element (pixel).  $k$  is estimated as:

$$k = 0.046 \cdot LAI \quad (2-8)$$

The value of  $Int$  can never exceed the interception storage capacity, which is defined as the difference between  $S_{max}$  and the accumulated amount of water that is stored as interception,  $Int_{cum}$ .

In LISFLOOD the simulation of preferential bypass flow –i.e. flow that bypasses the soil matrix and drains directly to the groundwater is carried out by:

$$D_{pref,gw} = W_{av} \left( \frac{w_1}{w_{s1}} \right)^{C_{pref}} \quad (2.1.1)$$

Where  $D_{pref,gw}$  is the amount of preferential flow per time step[mm],  $W_{av}$  is the amount of water that is available for infiltration, and  $C_{pref}$  is the empirical shape parameter, which is used as a calibration constant. The equation results in a preferential flow component that becomes increasingly important as the soil gets wetter. The actual infiltration  $INF_{act}$  [mm] per time step is now calculated as:

$$INF_{act} = \min(INF_{pot}, W_{av} - D_{pref,gw}). \quad (2.1.2)$$

Finally, the surface runoff  $R_s$  [mm] is calculated as:

$$R_s = R_d + (1 - f_{dr}) \cdot (W_{av} - D_{pref,gw} - INF_{act}) \quad (2.1.3)$$

Where,  $R_d$  is the direct runoff (generated in the pixel's 'direct runoff fraction'). Equation (2.1.3) thus gives the surface runoff for the whole pixel (pervious+impervious fraction).

As far as we know there is no general equation that accounts for preferential bypass flow, but ignoring it completely will lead to unrealistic model behavior during extreme rainfall conditions. Equation 2.1.1 is a very simple approach used in LISFLOOD. During each time step, a fraction of the water that is available for infiltration is added to the groundwater directly (i.e. without first entering the soil matrix). It is assumed that this fraction is a power function of the relative saturation of the topsoil (van derKnijff et al., 2008, van der Knijff and de Roo, 2008).

In LISFLOOD the simulation of fast subsurface flow through macropores (preferential flow), it is assumed that the fraction of the water on the soil surface contributing to preferential flow is a non-linear function of the relative saturation of the topsoil, and that the importance of preferential flow increases as the topsoil gets wetter. For the remaining water that falls on the soil surface, infiltration and surface runoff are simulated using the Xinanjiang approach (Zhao & Liu, 1995; Todini, 1996). The moisture fluxes out of the top- and subsoil are calculated assuming that the flow is entirely gravity-driven. The groundwater system is described using two parallel interconnected linear reservoirs, similar to the HBV-96 model (Lindström et al., 1997). The upper zone represents a mix of fast groundwater and subsurface flow, including flow through macropores. The lower zone has a much slower response and generates the base flow. Routing of water through the river channel can be simulated with the kinematic or the dynamic wave descriptions (Chow, 1988). Whenever possible parameters in LISFLOOD are linked to physical properties, e.g. soil or landuse properties, however, default values for five parameters are proposed but need to be calibrated for better model performance (Feyen, 2005, van der Knijff and de Roo, 2006). Analysis of model parameter uncertainty and its impact on discharges simulated by the LISFLOOD model is presented in Feyen et al., 2007.

For this study the model has been set-up for a region including all basins with a 1 km<sup>2</sup> grid. Time steps are adapted to the resolution of the input variables available for this study. For the long term simulations these are daily and for the detailed case study calculations hourly. Since the aim of the study is to test the approach for ungauged river basins, the available discharge data have been used for comparison and validation only, and not for calibration. Instead, default values for the parameters have been used throughout the study (van der Knijff and de Roo, 2006, van der Knijff et al, 2008).

### **2.3. Input data**

For the determination of the hydrological regime over the past years, synoptic meteorological station data from the data archive of the AgriFish<sup>1</sup> unit at the DG Joint Research Centre have been used. Their database holds reliable meteorological data from about 2000 stations across Europe since 1990. In the areas under study the meteorological stations are available for which daily values of temperature and rainfall have been reported and potential evaporation estimated.

High-resolution operational weather forecasting data are provided to the JRC for research by the German national weather service (DWD). In 2002 the Local model of the DWD had a grid spacing of 7 km, an hourly temporal resolution, and a forecasting lead time of 48h. The DWD forecasts are provided every 12 hours starting at 00UTC and 12UTC.

---

<sup>1</sup> <http://agrifish.jrc.it>





## 2.4. Methodology of discharge threshold exceedances

In order to issue a flood warning a decision making element needs to be incorporated: is the discharge going to exceed a critical threshold or not? The determination of the critical thresholds is crucial, in particular when dealing with watersheds where only few or no discharge measurements are available. For this study a model consistent approach which has been tested previously for early flood warning in large river basins (Ramos et al., 2007, Thielen et al, 2007) is proposed:

- 1) A long time series simulation based on observed meteorological data is calculated with LISFLOOD. Obviously, the denser the station network, the better rainfalls and subsequent discharge peaks can be captured.
- 2) For each grid point, the discharges from the long-term time series are evaluated statistically for threshold values, e.g. for return periods or quantiles. Due to the relatively short time series for which reliable meteorological data are available for this study (1990 to 2002) – the quantiles approach was used. Discharges are ranked from highest to lowest and certain cut-off values chosen as thresholds. The highest discharge is defined as the *severe* threshold level. The one corresponding to the 99% highest discharge is chosen as the *high* threshold level (comparison with observations has shown that this corresponds frequently with observed 1-2 year return periods), the 98% as medium and 97% as low.
- 3) Comparison with observations is performed through exceedance of critical thresholds, e.g. is  $Q_{obs} > Q_{critical\ obs}$  when  $Q_{sim} > Q_{critical\ sim}$ , for each available station.

The major advantage of this approach is that any systematic over- or under-prediction of the model is compensated for. If the model tends to overestimate discharges in a given river reach, for example because of a non-optimized parameterization or lack of processes such irrigation or reservoir operations, this would be reflected in the thresholds as well as in the forecasts. In this way the relative difference of simulated discharge to simulated thresholds but not the actual values are evaluated. The same procedure was used for the calculation of observed thresholds. For visualization, the critical thresholds are coded by different colors (Table 1).

Table 1: EFAS thresholds, their color codes and associated hazard class

EFAS threshold	Color	Description
<b>S (Severe)</b>		Very high possibility of flooding, potentially severe flooding expected
<b>H (High)</b>		High possibility of flooding, bankfull conditions or higher expected
<b>M (Medium)</b>		Water levels high but no flooding expected
<b>L (Low)</b>		Water levels higher than normal but no flooding expected

For those stations where observed discharge data are available, the same method has been applied to calculate the corresponding critical values  $Q_c$  obs.

One of the major drawbacks for this study lies with the different time and space resolutions that are imposed by the availability of the data. While for the determination of the thresholds only daily meteorological and hydrological data are available over a sufficient long time, flashfloods themselves develop on shorter time scales. It is therefore likely that the calculated thresholds are low compared to the actual peak discharges occurring during flashfloods. In a similar way, the weather forecasting data neither entirely match the resolution of the climatological network nor the high-resolution network. Too low thresholds can lead to a high number of false alarms that could be reduced if the data used to determine the thresholds were of higher resolution. For the purpose of this study, which focuses on early warning for flashfloods, the low threshold values do not necessarily pose a problem as long as the exceedance of the high and severe thresholds is taken as indication only that flashfloods are likely. Quantification and localization of these warnings would have to be confirmed through real-time rainfall measurements with gauges and radar.

### 3. Case studies

#### 3.1. The flash flood event 8-9th September 2002 – France

##### 3.1.1. The Cévennes - Vivarais region in Southern France

The Cévennes-Vivarais region (Fig. 3.1.1.1) is situated Southeast of the Massif Central, the V-shaped Hercynian mountain range of the central part of France (85000 km<sup>2</sup>; i.e. one sixth of the country area). The relief is a southeasterly facing slope starting from the Mediterranean shore and the Rhône Valley. The altitude of the mountain range varies from sea level up to 1700m (Mount Lozère) over roughly 70km. The area is characterized by relatively small catchments (few hundreds of km<sup>2</sup>) with short response time of less than 12 hours. The main Cévennes Rivers are Virdourle, Ardèche, Cèze, and Gard. They are characterized by a typical Mediterranean hydrological regime with very low level of water in summer and floods occurring mainly during the autumn. Figures 3.1.1.2 and 3.1.1.3 illustrate that most of the floods takes place during the autumn and winter months from September to February.

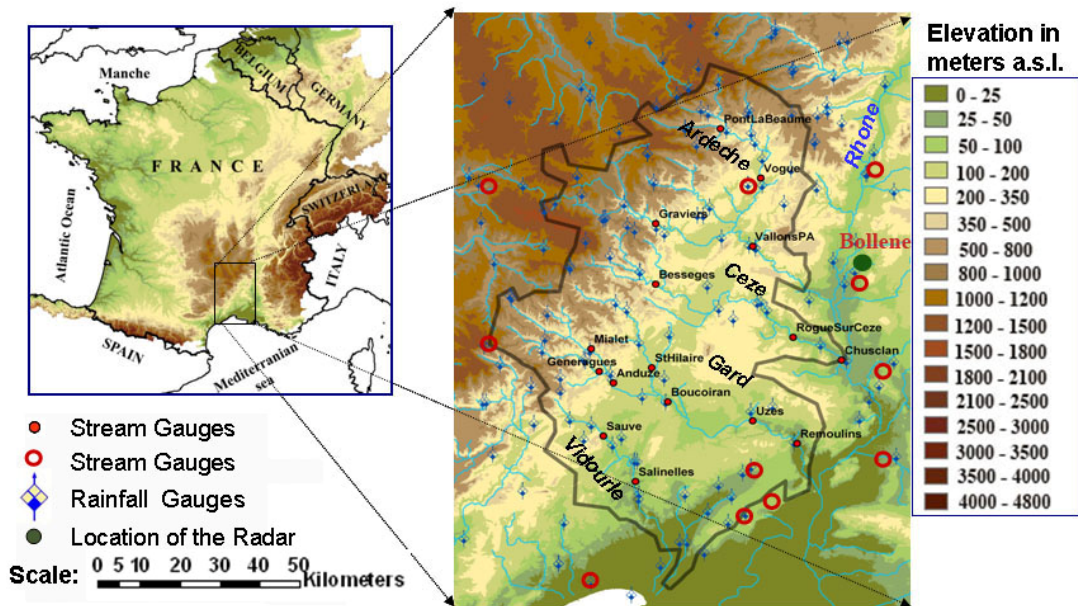


Figure 3.1.1.1: Map of the topography of France and zoom into the study area of the Cévennes region with the catchments used for this study. Rainfall gauges from high density network (hourly data, blue flags), stream gauging stations (red dots), and synoptic meteorological stations (daily data, red circles). The location of the Bollene radar is also indicated in the map.

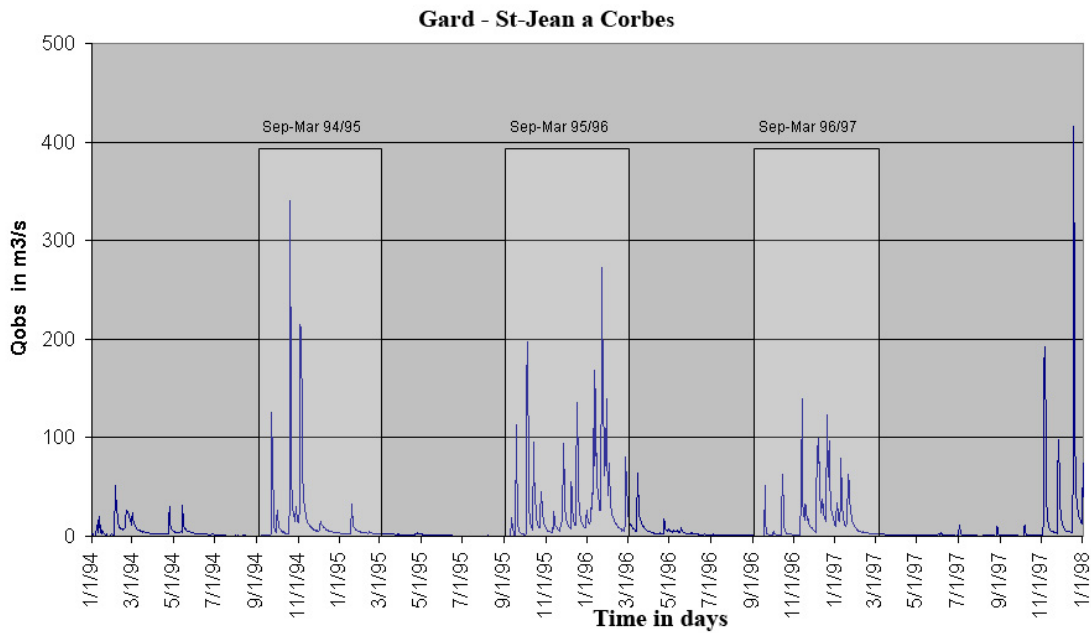


Figure 3.1.1.2: Shows that major floods occur during autumn and winter seasons in Mediterranean region.

### Flood Events Above Observed High Threshold for Gard river at Generargues from 1991 to 2006

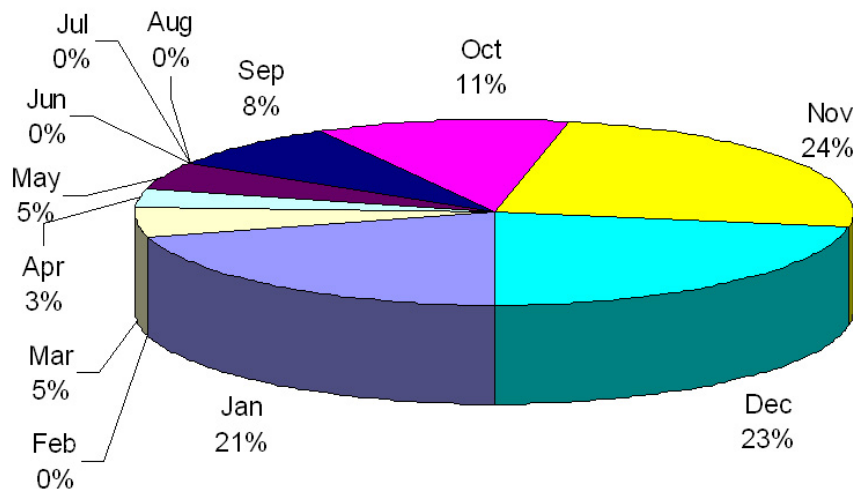


Figure 3.1.1.3: Distribution of observed flood events over the months for Gard River at Generargues stream gauging station from 1991 to 2006.

For this study four watersheds are analyzed, the Ardeche, the Ceze, the Gard and the Vidourle. The outlets at which comparison of observed with simulated data are performed are listed in Table 2. Only those meteorological and hydrological stations with long-term records from 1990 to 2002 were chosen. In total, 11 meteorological stations and 15 discharge stations were selected (Fig. 3.1.1.1). Radar information was used from the 2002.09.08 06:00 onward for a period of 36 hours.

Table 2: This table shows the list of river basins, discharge stations and their upstream areas used in this study. In addition the observed maximum daily discharge (Qmax) for the study period 1990-2002 is given, the recorded maximum discharge at this station (Qmax\_recorded) and at what date, the 2, 5 and 10 year observed return periods (RP2,5,10 yrs), and the high threshold calculated from the observed daily discharges.

Basin	Station	Upstream area [km <sup>2</sup> ]	Q <sub>max,(1990-2002)</sub> /Q <sub>max_recorded</sub>	Q <sub>obsHigh</sub> (1990-2002)
			RP <sub>2 yrs</sub> /RP <sub>5 yrs</sub> /RP <sub>10 yrs</sub> [m <sup>3</sup> /s]	[m <sup>3</sup> /s]
Ardeche	Ard102-Pont de Labeaume - V5004010	264	404 /531(8/11/82)	134
			220/320/390	
	Ard105-Vogue-V5014010	636	830/890(23/10/77)	233
			420/600/720	
Ardeche	Ard501-Chambonas-V5045020	476	608/878(10/11/76)	118
			280/450/570	
Ceze	Ceze102-Besseges-V5424010	230	262/475(23/10/77)	64
			130/200/250	
	Ceze104-Roque_sur_Ceze-V5474010	1060	1170 /1200(24/10/77)	171
			410/670/840	
Ceze	Ceze106-Chusclan-V5474020	1180	1250 /1250 (21/10/94)	209
			-/-/-	
Gard	GAR103-Corbès-V7135010	263	416/510(23/10/77)	94
			150/230/280	
	GAR104-Généragues-V7124010	251	353/450(23/10/77)	82
			150/220/270	
GAR203-St. Hilaire-Brethmas - V7155040	328	302 /302(20/10/94)	88	
		-/-/-		
GAR301-Boucoiran-V7164010	1087	424 / (no info)	236	
		-/-/-		
Vidourle	Vid103-Le Vidourle a Sauve-Y3414010	190	417 (9/9/2002)	47
			120/180/220	
Vidourle	Vid105- Le Vidourle a Salinelles – Y3444010	539	978 ((no info)	63

- total gap in data records >3 years; \*\* total gap in data records 3 < years < 6; \*\*\* total gap in data records > 6 years



### 3.1.2. Description of the 8-9th September 2002 case study

The 8-9 September 2002 heavy precipitation event was responsible for one of the most important floods ever recorded in the Cévennes–Vivarais region. It caused 24 casualties and an economic damage estimated at 1.2 billions euros (Huet et al., 2003).

The event started early in the morning of the 8th September 2002 with first convective cells forming over the Mediterranean Sea. The convection progressed northward to form inland a mesoscale convective system over the Gard). The quasi-stationary system stayed over the same region until approximately the next morning, and then evolved eastward together with a surface front. For more detail on the event refer to (Delrieu et al., 2005). For the whole event, the raingauge network locally recorded 24h cumulated rainfall greater than 600mm (Fig. 3.1.2.1a), which is confirmed by the radar observation (Fig. 3.1.2.1b).

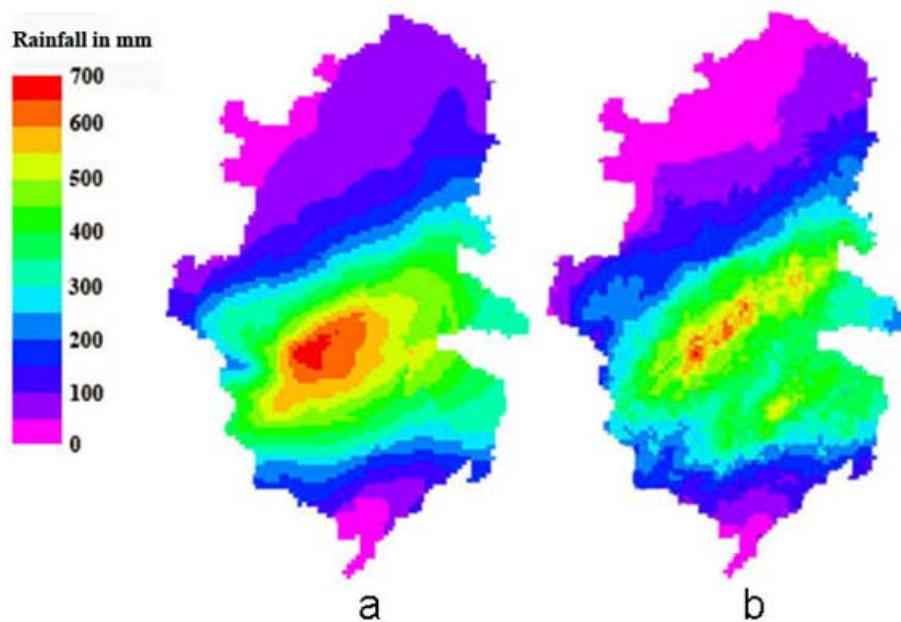


Fig. 3.1.2.1: Accumulated 48 h observed rainfall from 20020908 as observed by gauges (a) and by radar (b). Locations of the gauges used for the interpolation are shown in Figure 3.1.1.1.

For the Gard and Vidourle river watersheds, the peak discharges were observed to be two times higher than the ten years return period specific discharge (Delrieu et al., 2005; Chancibault et al., 2006). In Fig. 3.1.2.3, the maximum specific discharge recorded or retrieved from a post-event field experiment (Delrieu et al., 2005) presents the intensity of the hydrological response of the watershed within the region. In Figure 3.1.2.3, most of the estimated peaks indicate specific discharges of more than  $5 \text{ m}^3\text{s}^{-1}\text{km}^{-2}$ , with some of them over  $20 \text{ m}^3\text{s}^{-1}\text{km}^{-2}$ . These are the most important values ever reported for watersheds of similar areas in France (Delrieu et al., 2005). The 10 years return period discharge for such catchments is about  $2 \text{ m}^3\text{s}^{-1}\text{km}^{-2}$  in this region. This figure also points out the characteristic size of the watershed affected by the flood for which detailed rainfall fields have to be correctly forecasted.

A more detailed description of the case study can be found in Delrieu et al. (2005), Chancibault et al. (2006) and Nuissier et al. (2007).



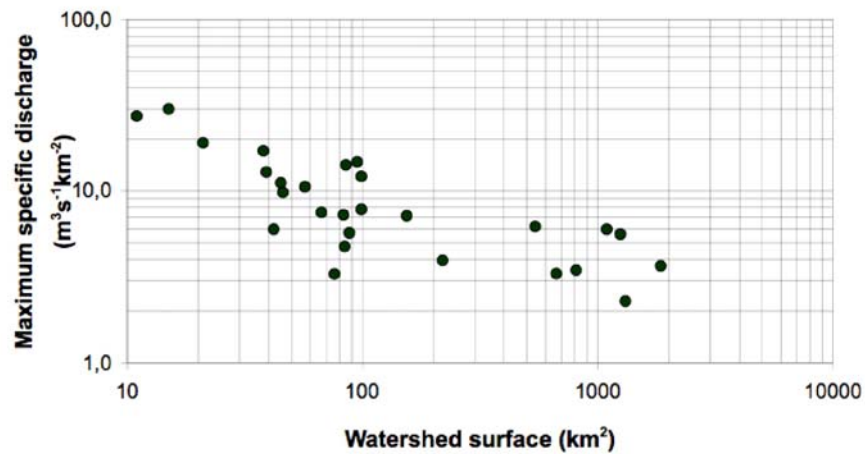


Fig. 3.1.2.3: Observed maximum specific discharges for the flash flood event in September 2002 in the Cévennes-Vivarais region. The plot is based on the data collected in the post-event field experiment as described in Delrieu et al. (2005).

### 3.1.3. Input data for the study

For the determination of the hydrological regime over the past years, synoptic meteorological station data from the data archive of the AgriFish<sup>i</sup> unit at the DG Joint Research Centre have been used. Their database holds reliable meteorological data from about 2000 stations across Europe since 1990. In the study area 11 meteorological stations are available for which daily values of temperature and rainfall have been reported and potential evaporation estimated (Figure 3.1.3.1).

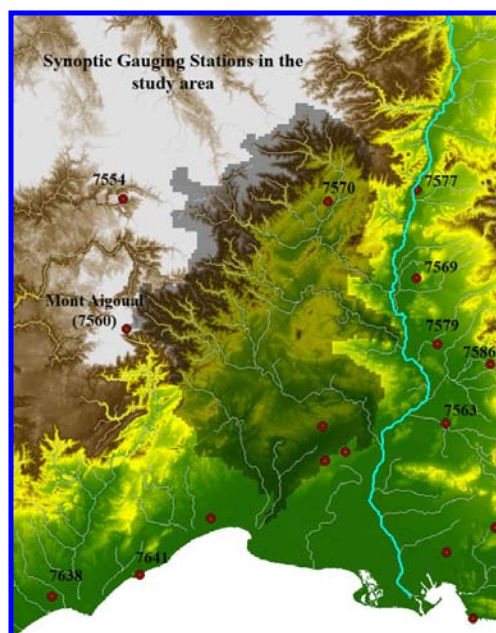


Fig. 3.1.3.1: Distribution of synoptic meteorological stations in the study area used for long term simulation for threshold calculation.

For the case study hourly meteorological and hydrological data are available from the databank of the Observatoire Hydrométéorologique Méditerranéen - Cévennes – Vivarais (OHM<sup>2</sup>-CV) which has been initiated in 2000 to understand intense Mediterranean storms that lead to devastating flash floods.

Rainfall data estimated from radar was derived from the Bollène 2002 experiment (Chapon, 2006; Boudevillain et al., 2006) designed by DSO/Météo-France and LTHE. This experiment aimed at evaluating the benefit of a radar volume-scanning strategy (8 elevation angles in 5mn) for radar quantitative precipitation estimation in the Cévennes-Vivarais region. The 3 Plan Position Indicators (PPIs) corresponding to the elevation angles needed for the operational products in real time of the Bollène radar (Météo-France; Fig. 3.1.1.1) were complemented by two sets of 5 PPIs (elevation angle from 0.4° to 18°), alternated every 5mn. This protocol allowed a good sampling of the atmosphere at a 10mn sampling interval. The data available at 1x1km<sup>2</sup> resolutions were the average reflectivity and the mean absolute reflectivity difference averaged over the individual radar polar bins which centers fall within the corresponding Cartesian mesh. Innovative algorithms were developed in order to identify and correct various errors sources in quantitative precipitation estimation in mountainous regions (i.e. radar calibration, ground clutter identification, vertical profile of reflectivity versus rainfall). Calibration based on rainfall observations has not been used. For more details on each step of the radar data treatment see Boudevillain et al. (2006).

High-resolution operational weather forecasting data are provided to the JRC for research by the German national weather service (DWD). In 2002 the Lokalmodell of the DWD had a grid spacing of 7km, an hourly temporal resolution, and a forecasting lead time of 48h. The DWD forecasts are provided every 12 hours starting at 00UTC and 12UTC.

For the long-term simulations discharge data from 15 stream gauging stations were selected from the Banque d'Eau<sup>3</sup>, the French National database for discharge. At these stations discharge records are available from 1990 onwards. Only those stations were selected where the influence of hydrological structures such as reservoirs, can be assumed to be little. In addition, for 12 out of these 15 stations, also hourly data are available from the OHM-CV for the 2002 event.

#### **3.1.4. Hydrological regime and calculation of thresholds**

The hydrological regime of the river basins in the Cévennes-Vivarais region is illustrated in Fig. 3.1.4.1 which illustrates the concentration of peak discharges in autumn and spring for the two catchments Gard and Ceze. Despite the coarse meteorological station network data used as input, the simulations capture the periods of high flows reasonably well. Although peaks are both over- or underestimated, the scatter plot in Fig. 3.1.4.2 shows clearly that the model rather tends to underestimate the discharges. Particularly severe is the underestimation of simulated discharge in the example of the Ardèche.

---

<sup>2</sup> <http://www.lthe.hmg.inpg.fr/OHM-CV>

<sup>3</sup> <http://www.hydro.eaufrance.fr>

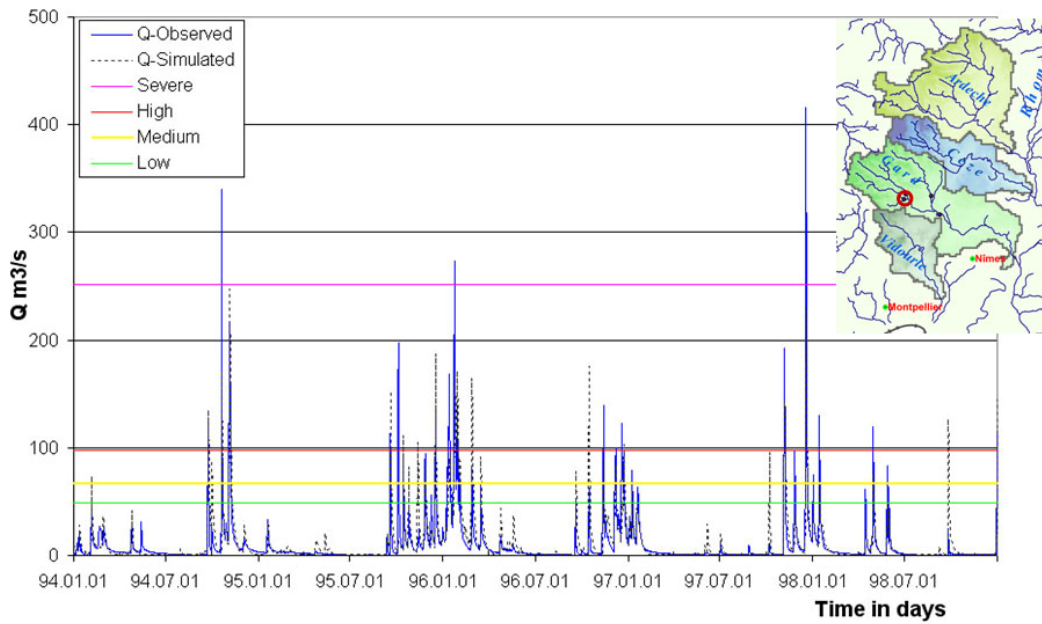


Fig. 3.1.4.1a: Observed (Blue) and simulated (black) Gard discharges at station Corbès (262 km<sup>2</sup>) from 1/1/1994 to 31/12/98.

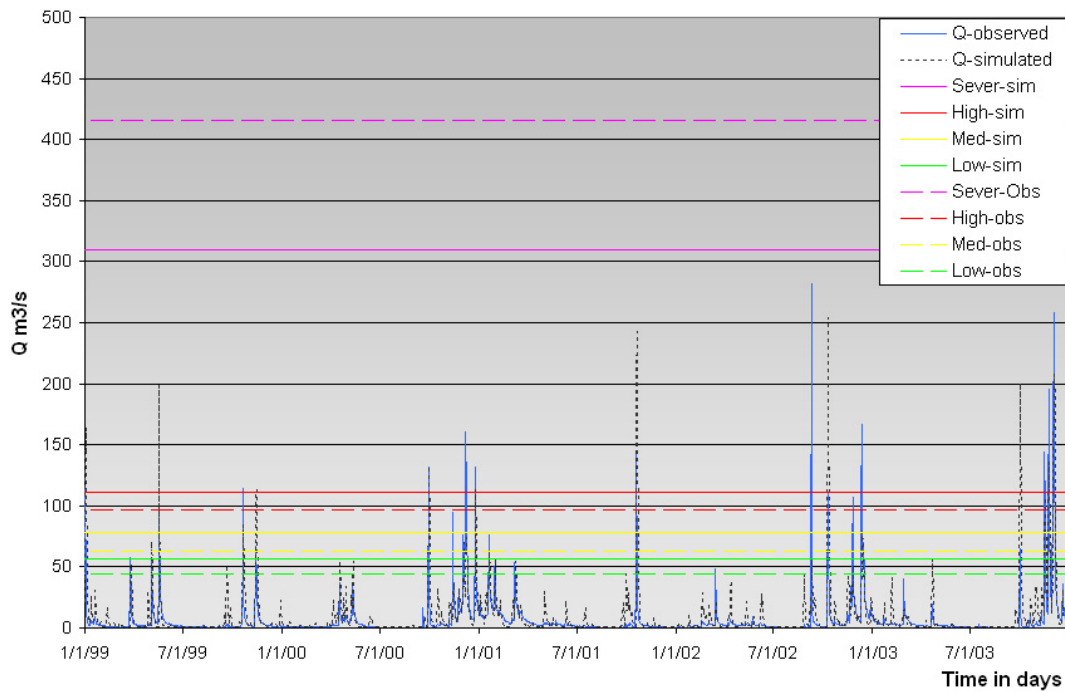


Fig. 3.1.4.1b: Observed (Blue) and simulated (black) Gard discharges at station Corbès (262 km<sup>2</sup>) from 1/1/1999 to 31/12/2003, taking into account the difference in threshold.

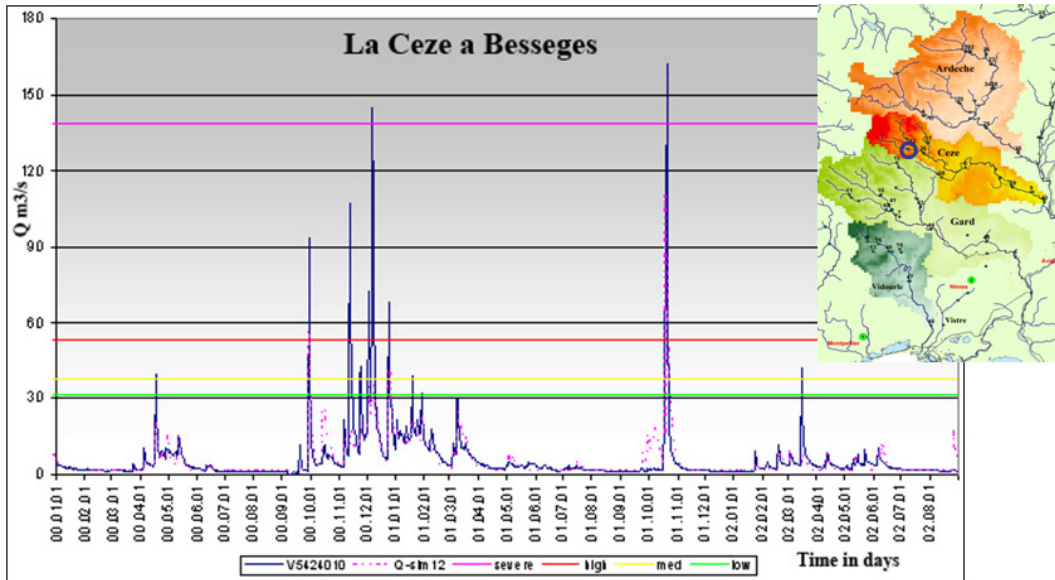


Fig. 3.1.4.1c: Observed (Blue) and simulated (pink) Ceze discharges at station Besseges (230 km<sup>2</sup>) from 1/1/2000 to 31/12/2002.

As emphasized before, it is not the absolute discharges that are of interest in this study but the exceedance of corresponding thresholds. Comparison of the number of threshold exceedance between simulations and observations yield similar results over the 12 year period (not shown), indicating that the chosen time interval for the calculation of thresholds is sufficiently long.

The exceedances of threshold levels for both the simulated and observed discharges have been summarized in contingency tables (Table 3) for each of the four threshold levels. Figure 3.1.4.3 shows, for the same stations as in Figure 3.1.4.2, the first three components of this contingency table for thresholds high, medium and low. By definition, the “severe” threshold, which is defined as the highest discharge of the time series, cannot be exceeded and is therefore zero in all cases. Positive rejections, the vast majority of the cases, are not plotted to avoid distortion of the graphs.

The splitting of the contingency tables shows mixed results. When analyzing the data according to the lowest alert class, there are generally more hits than false alarms or misses. The number of misses and false alarms is about equally high. When looking in more detail at the different threshold classes, the results worsen as the severity class increases. These results have, of course, to be analyzed in view of the quality of the meteorological input data and the events analyzed. Flash floods are events that are much localized and there is a high probability that the synoptic station network misses the event – hence a high number of misses. More surprisingly is perhaps the high number of false alarms. This can be partially explained with the temporal resolution of the input data and the corresponding daily time step which can easily introduce a 1 day time shift which in this rigid analysis based on daily values then counts as a miss or false alarm. If the input data was available at a higher temporal resolution and derived from a higher density network, the results would very likely be better. It can be concluded from the long-term study that with the given input data resolution the simulated discharges tend to be considerably lower than the observed ones. Therefore quantitative analysis of discharges could not be used for flood warning, while the threshold exceedance approach allows better identification of events.

The number of threshold exceedances, shown in Figure 3.1.4.4 as cumulative values over the 12 year period for both simulated and observed data series, shows that the simulated threshold exceedances compare well with the observed ones, in particularly for the Gard and Ardeche. While during certain periods differences can occur, with increasing number of years the values approach similar numbers, indicating that the 12 year period is sufficiently for the calculation of the thresholds.

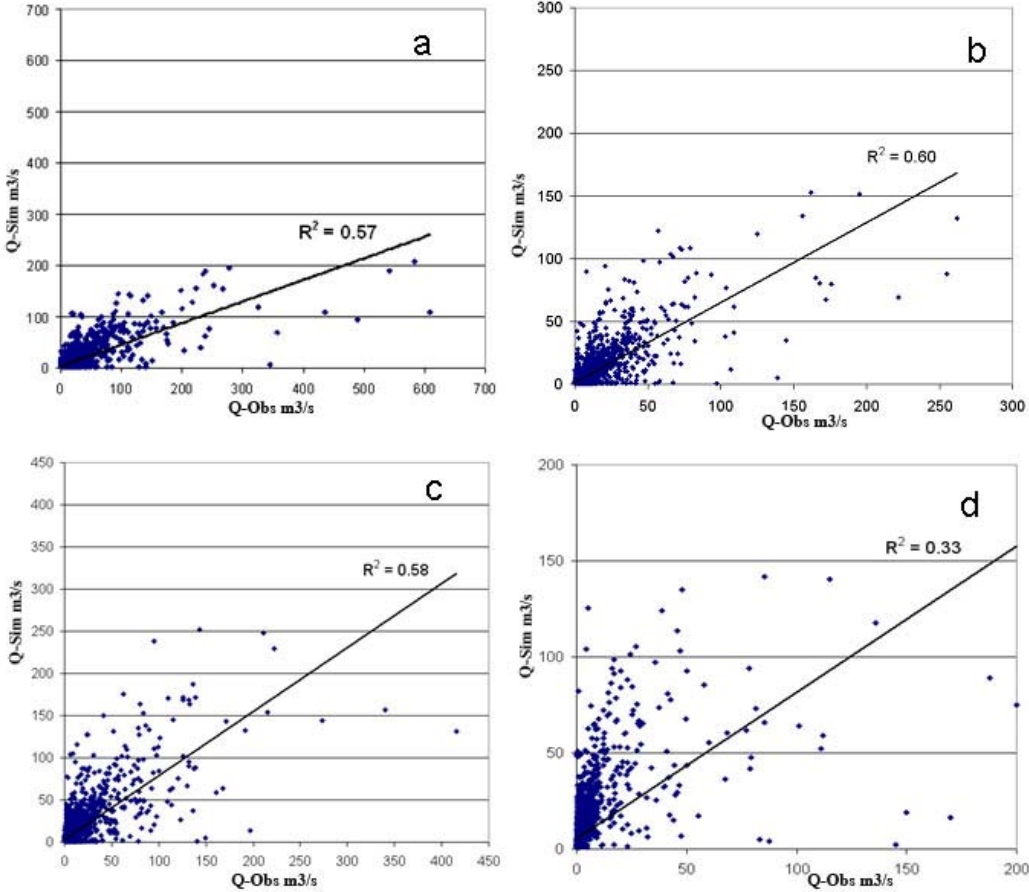


Fig. 3.1.4.2: Scatter plots for the stations in the Ardèche (a), Cèze (b), Gard (c) and Viridourle (d) with the daily observed discharges in m<sup>3</sup>/s on the x-axis and simulated discharges in m<sup>3</sup>/s on the y-axis during the 1990 to 2002.

Table 3: Definition of contingency table

	$Q_{obs} \geq Q_{c\ obs}$	$Q_{obs} < Q_{c\ obs}$
$Q_{sim} \geq Q_{c\ sim}$	H (Hit)	F (False)
$Q_{sim} < Q_{c\ sim}$	M (Miss)	PR (Positive Rejection)

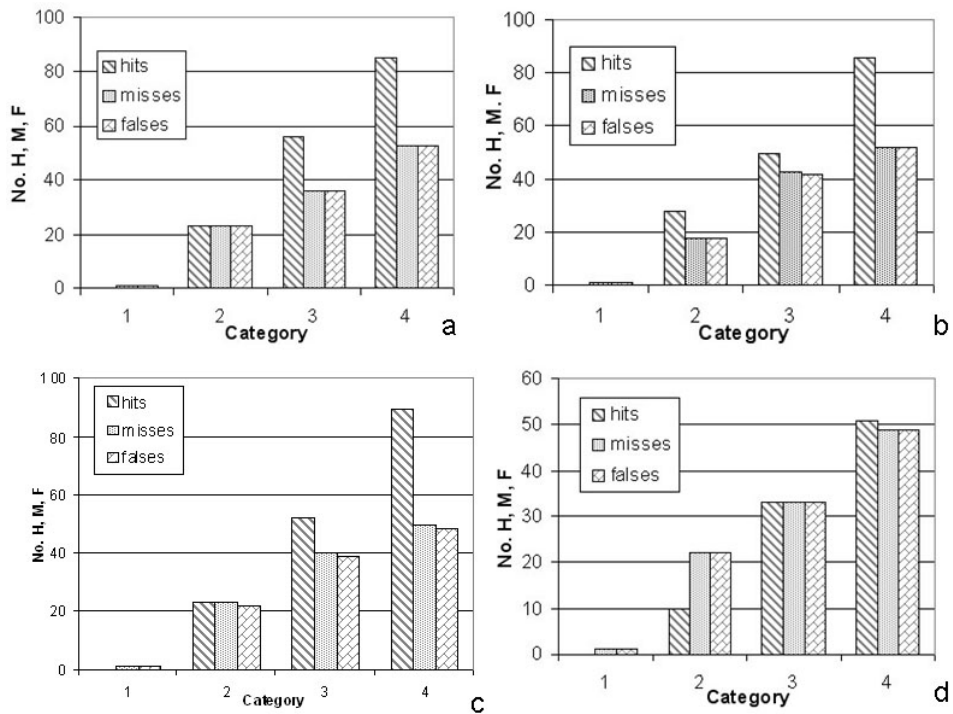


Fig. 3.1.4.3: Contingence tables of hit, false, and missed threshold exceedances for Gravière in the Ardeche (a), Bessège in the Cèze (b), Corbès in the Gard (c) and Sauve in the Virdourle (d) for the daily discharge exceedance analysis from .1990-2002.

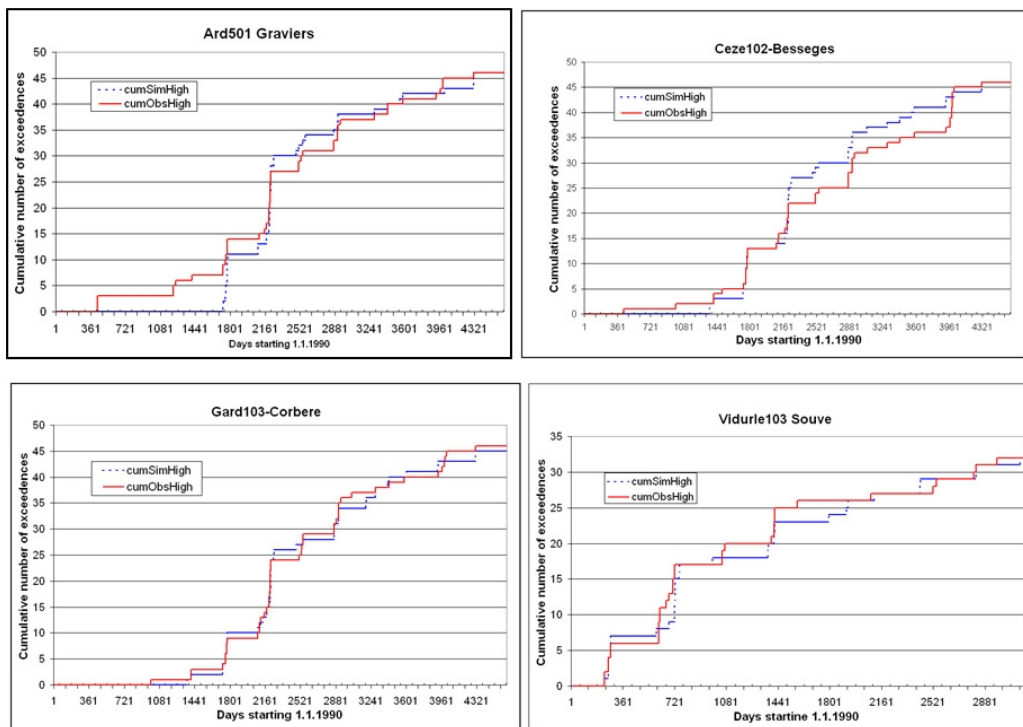


Fig. 3.1.4.4: Cumulative number of threshold exceedances for the observed (solid) and simulated (dashed) time series starting on 1.1.1990 up to 31.12.2001.



### 3.1.5. Forecasting the 8-9th September 2002 event

In LISFLOOD the output of the daily long-term simulations are used as initial conditions for the hourly flood simulations.

Comparison between accumulated rainfalls from radar (Fig. 3.1.2.1), high resolution rain gauge network and weather forecasts (Fig. 3.1.5.1) show that there are big differences in terms of spatial distribution as well as magnitude.

Taking the high resolution rainfall network data as reference, Fig. 3.1.2.1 shows that the radar produced very similar rainfall in terms of quantity and spatial distribution. There is more information on the spatial variability in the radar data as compared to the interpolated gauge data. In contrast, the daily values of the synoptic gauges do not capture the event in its total spatial distribution. The rainfalls are concentrated in the Southeast of the catchment. Also the rainfall quantity is much too low. As for the weather forecasts, the rainfall patterns are shifted too far north as compared to the observation. This is has been observed also for other meteorological models as documented in Anquetin et al. (2005). Also, the overall volume of precipitation has been underestimated by the weather forecasting model, which again has been observed previously for other weather forecasting models.

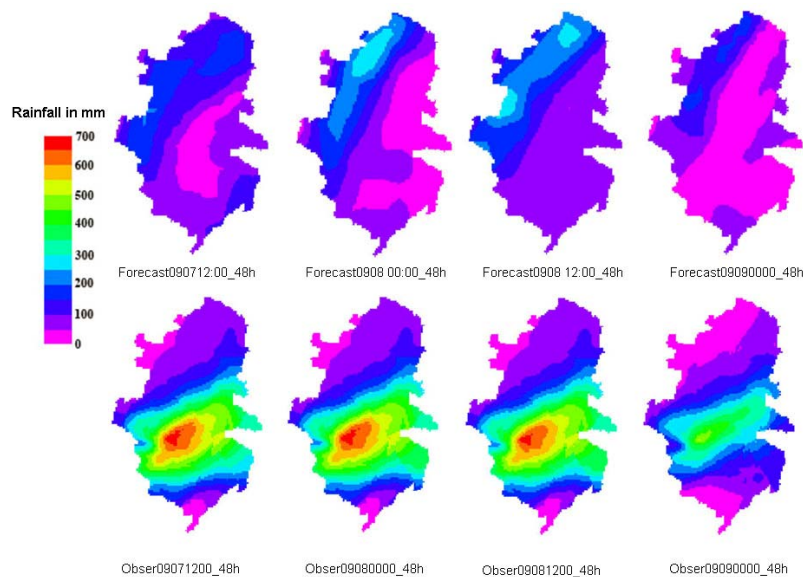


Fig. 3.1.5.1: Accumulated rainfalls from the 20020907 12:00 20020908 00:00, 20020908 12:00 20020909 and 00:00 48 hours forecasts, and observed (using 101 rainfall gauging stations (see figure 3.1.1.1) for the same period.

Fig. 3.1.5.2a shows hourly hydrographs based on the radar estimated rainfall and high density rain gauge network. Both simulated discharges are compared against the observed discharge at Générargues in the Gard River. In Fig. 3.1.5.2b, the hourly simulated discharges are based on the 7-km resolution weather forecasts from the German National Weather Service at the same outlet.

This graph clearly illustrates the principle of the threshold exceedance. The simulated discharges – even with high resolution radar and gauge data – are 3 times lower than the observed discharges they are reaching (radar) or exceeding (gauges) the EFAS severe

threshold indicating serious flooding in the Gard. Although the forecasted rainfalls for the region were shifted too far north compared to the observations and comparatively low rainfalls were forecasted over the Gard basin (Fig. 3.1.5.1), the high threshold is being exceeded with all forecasts from the 07th September 12:00 forecast onwards. Also the timings of the forecasted peaks correspond well with the observed peak on 9th September at 6:00 o'clock +/- 1-2 hours. Thus, although the severity of the event is underestimated, there is an early warning indication that flooding can be expected within 42 hours. Estimating the runtimes of the meteorological and hydrological models as well as data transfer and preparation time of the data to about 6 hours, the leadtime is still of the order of 1 day and more (Fig. 3.1.5.2c). In contrast to the Gard basin, the discharge forecasts for the Ardeche overestimated the severity of the event (Fig. 3.1.5.3). Clearly, the benefit of these forecasts lies with the potential early warning of the flood event. As the events draw nearer, the flood forecasters would increasingly make use of the observational networks to identify the spatial distribution and the magnitude of the flooding.



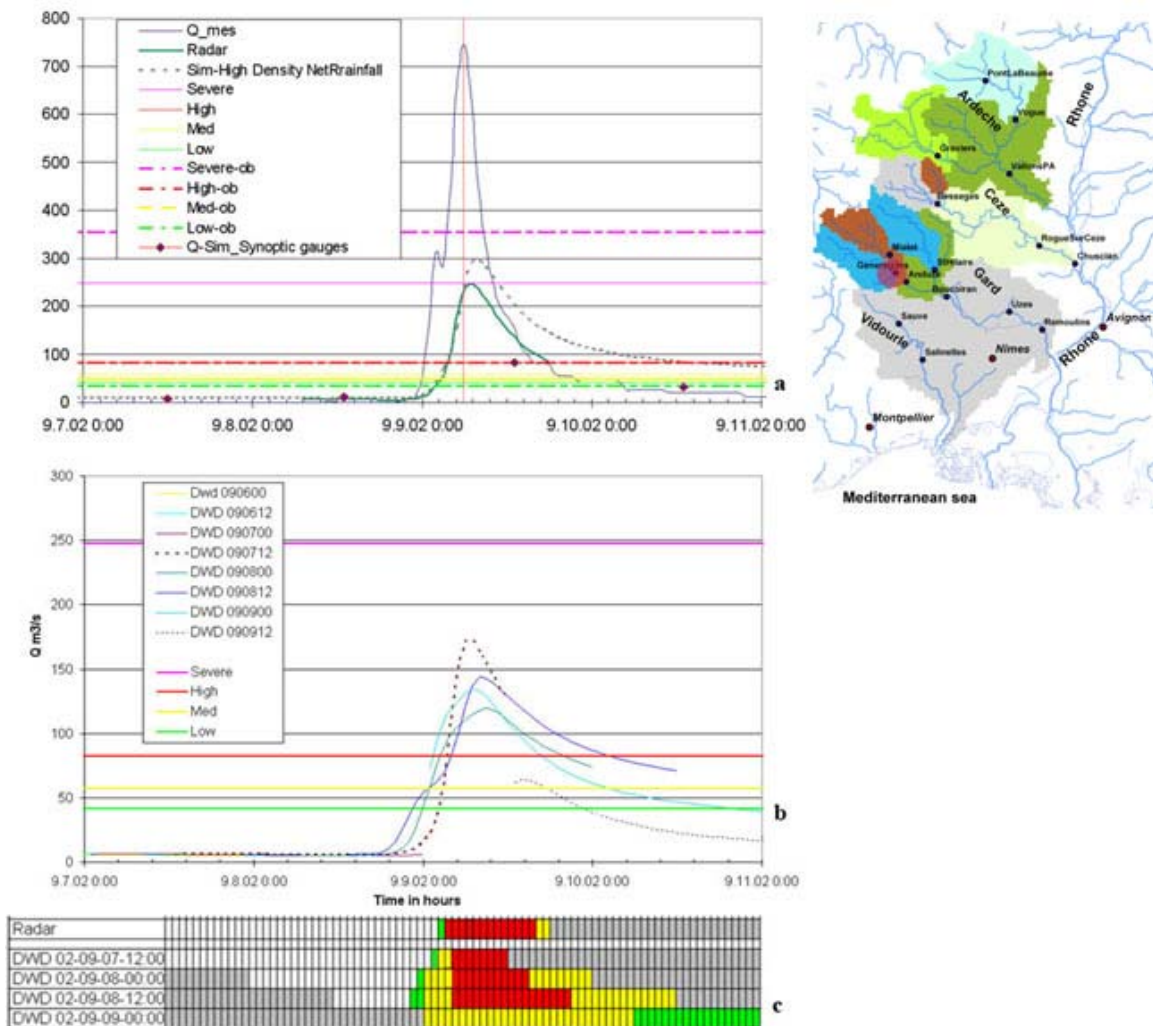


Fig. 3.1.5.2: a- Observed hydrograph at Générargue in the Gard river with the vertical line indicating the time of peak at 06:00 on 9th September, while at 07:00 with Radar(Green) and at 08:00 with the using of high density rainfall gauging network (Grey dashed). b- Hydrographs of forecasted discharges in m<sup>3</sup>/s (y-axis) for Générargue (244 km<sup>2</sup>) in the Gard river from the 9th-12th Sep 2002 starting at 12:00 in hourly time steps (x-axis). The flood forecasts based on DWD forecasts start on 0906 00:00 until 0909 00:00 in 12h time intervals. c- illustrates the visualization of threshold exceedances in hourly time steps for the flood forecasts based on radar data and 48 hours DWD Lokalmodell forecasts from 20020907 00:00, 20020907 12:00, 20020908 00:00, 20020908 12:00 and 20020909 00:00. The exceeded thresholds are color coded as purple (severe), red (high), yellow (medium) and green (low). Grey color indicates no data available.

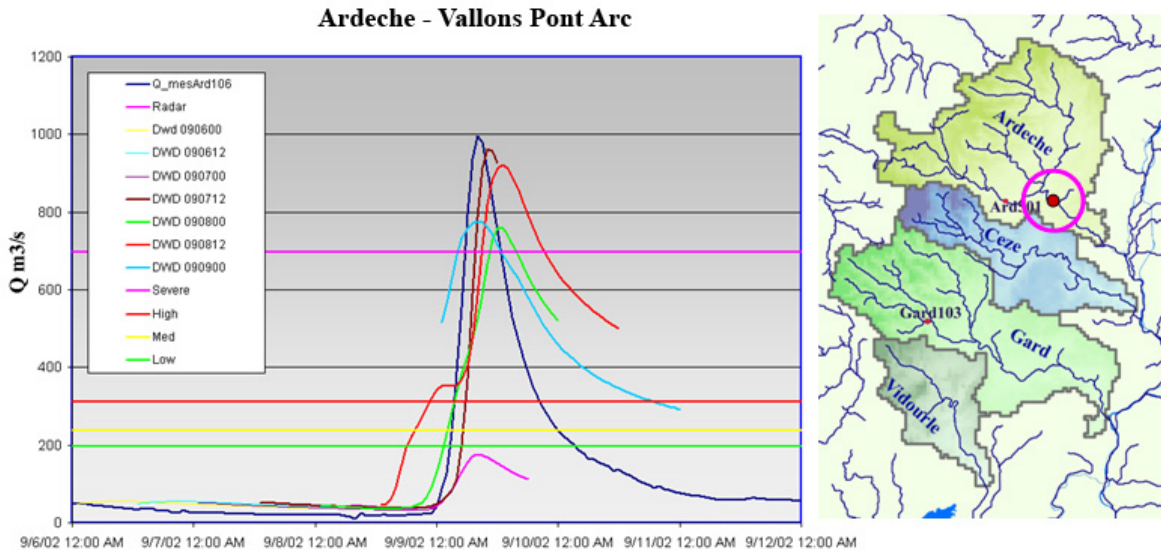


Fig. 3.1.5.3: Comparing observed discharge for Ardeche at Vallon Pont d’Arc (1930 km<sup>2</sup>) with Radar input rainfall data giving underestimation of the resulting discharge, while with the model consistent threshold, the severe threshold is reached with the forecast from 7<sup>th</sup> September 12:00 onwards.

Fig. 3.1.5.4 illustrates the spatial development of forecasted event. Again the exceeded alert thresholds are visualized with the colour coding listed in Table 1. Each panel shows the maximum alert threshold exceeded during the forecasting period in 12 hourly steps. The panel clearly illustrates that the event is first forecasted on the 07<sup>th</sup> 12:00 to take place in the upstream areas of all 4 river basins. In the next forecasts the emphasis is mostly in the Gard and Cèze rivers and less in Ardèche and Viridourle. The panel shows how the flooding is forecasted to affect almost the whole basins well exceeded the severe thresholds over large parts of the river basins. Downstream, towards the outlets, mostly only high thresholds are exceeded.

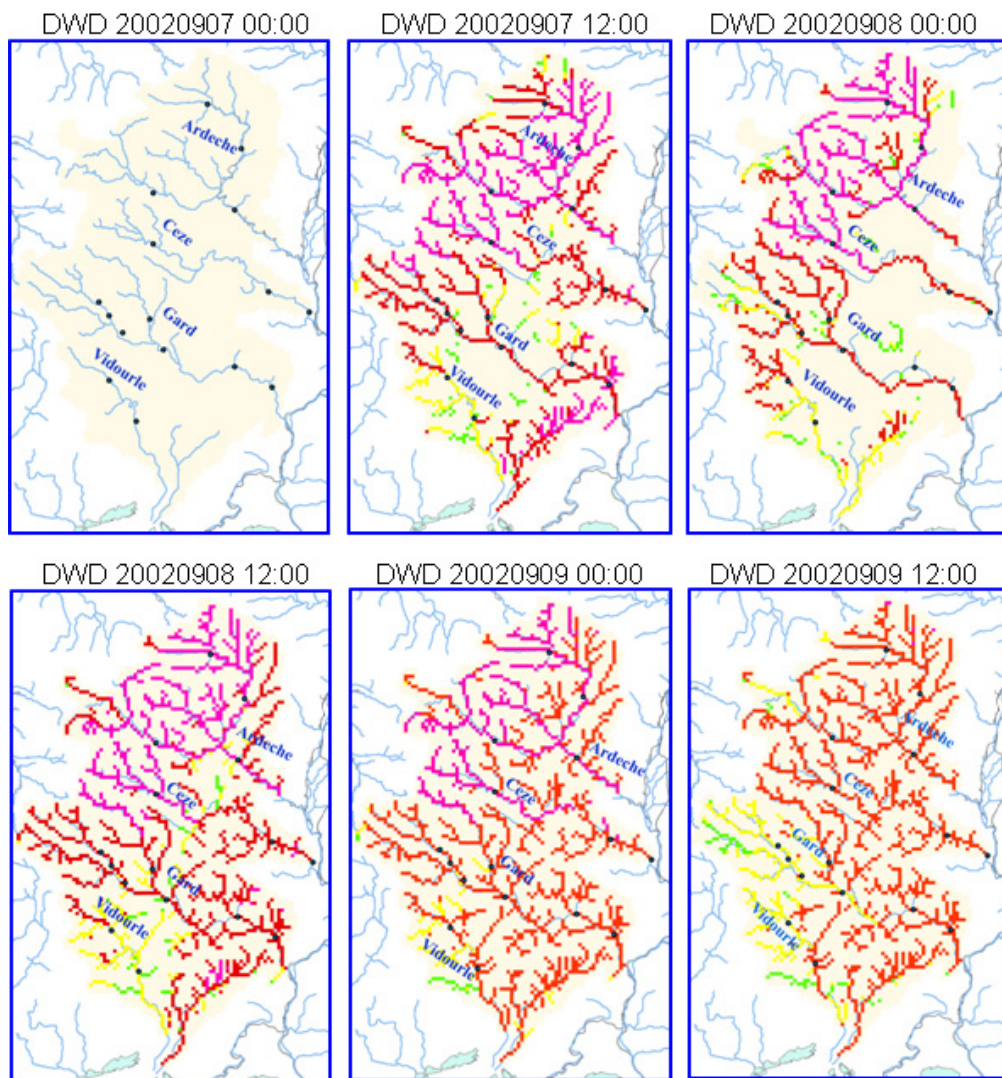


Fig. 3.1.5.4: Summary threshold exceedance maps showing the highest threshold exceeded during the 48 h forecasting time for flood forecasts based on the DWD Lokallmodell weather forecasts from 20020907 00:00 and in 12 hourly steps until 20020909 12:00. The threshold exceedances are color coded with purple (severe), red (high), yellow (medium) and green (low).

Compared to the images delivered by radar (Fig. 3.1.2.1) one can see that the spatial distribution of the event was well captured by the forecasts but that there was a tendency to shift the precipitations too far north. As a result, for example the Ardeche, was forecasted with more rainfall compared with observations while the Gard did not receive rainfall as much as observed. This is also reflected in the simulations.

In summary one can state that – in this particular case – system as the one presented could have provided early warning of the event to happen more than 24 hours in advance with a good estimation of areas affected, timing and magnitude of the event. It appears that the high thresholds derived from the long-term simulations can be used as indicator for flood events when limited area meteorological model input data are used to drive the simulations.

For this period the OHM-CV has classified 11 significant rainfall events (3, 5, 8-9 Sep, 9-10, 21, 30-31 Oct, 14,21 and 24 Nov and 10-11 and 27<sup>th</sup> Dec), where a significant event is defined when at least 1 station has reported more than 50 mm of rainfall during the event. Out of these 11 rainfall events 6 have resulted in a flood event (9 Sep, 10 Oct, 22 and 24-27 Nov, 11-13 and 29 Dec) where a flood event is defined as the observed discharge data having exceeded the observed high threshold.

Table 4 summarizes the number of hits, false alarms and misses for the period from 5<sup>th</sup> June 2002-31<sup>st</sup> December 2002. Positive rejections are not listed.

Table 4: Number of Hits, False Alarm and Misses out of 178 days of analysis from 5th June-31st December 2002 of flood forecasting based on the 12:00 DWD weather forecasting data.

	Hits	False Alarm	Misses
<b>June</b>	0	0	0
<b>July</b>	0	0	0
<b>Aug</b>	0	0	0
<b>Sep</b>	4	4	0
<b>Oct</b>	2	6	0
<b>Nov</b>	6	6	3
<b>Dec</b>	1	1	6
<b>Summary</b>	13	17	9

### 3.1.6. Assessments of hits, false alarms and missed events over a 6 months forecasting period

Having demonstrated for the case study that a threshold-exceedance system based on high-resolution operational weather forecasts is capable of detecting flash floods more than 24 hours in advance, the case study findings are supported by a 6 months analysis to assess the rate of alarms and missed events. For computational and data availability constraints this study is limited to running all 12:00 DWD forecasts for a six months period from June to December 2002. For the 6 months analysis only 9 out of the 15 stream gauging stations were available. For the assessment of the 6 months analysis a flood event is defined as the exceedance of the high alert threshold –simulated and observed correspondingly - at least once during a 24h period. If the high threshold has been exceeded during two consecutive days it is still only counted as 1 event. If the forecasted hydrographs exceed the simulated high threshold during any time of the observed event, it is counted as a hit.

Over the 6 months period there are more false alarms (17) than hits (13) and the number of misses is lowest with 9. From the table it seems striking that missed events occurred mostly in the winter months. A closer look at the December events showed that the weather forecasts were shifted too far north where more precipitation was simulated as snow than was observed. In some cases of false alarms the simulated thresholds were only slightly exceeded with the simulations while they just did not reach the observed thresholds. One of the reasons that the number of false alarms is higher than the hits is because the weather forecasts tend to spread the precipitation over larger areas than actually occur. As a result flooding was simulated in almost all river basins while it only occurred in 1 or 2. The threshold



method as presented in this paper does not show whether a threshold is only just exceeded or reached.

In terms of early warning the missed events are the most serious ones because they do not induce any precautionary measures, while early warning of false alarms can easily be identified through weather observations and radar prior to the event.

It can be concluded from the long-term study that a 6 months period for the statistical assessment of hits and false alarms is not long enough. The analysis indicates, however, that the method captures the major flood events, the forecasted rainfalls are often too wide spread resulting in a high number of false alarms. The number of missed events is comparatively low, which is important since missed events are the most undesired ones in terms of early flood warning.

The catastrophic 8-9 September 2002 Cevennes-Vivarais flash flood event was mainly controlled by the space-time structure of the rainfall and of the initial soil water content (Le Lay M. and Saulnier G.M., 2007). Within the European Flood Alert System, LISFLOOD produces daily soil moisture maps of Europe, which provide an instantaneous image of the current situation of the soil water content. The soil water content represented as soil suction (pF), its normalized value and the seven days trend maps, as well as time series for some selected regions are updated on a daily basis (G. Laguardia and S. Niemeyer, 2007). Figure 3.1.5.4, shows the high values of pF from June 2002, which refers to low soil moisture content, until 25<sup>th</sup> August. Afterwards the pF value for this region sharply decreases indicating high soil moisture.

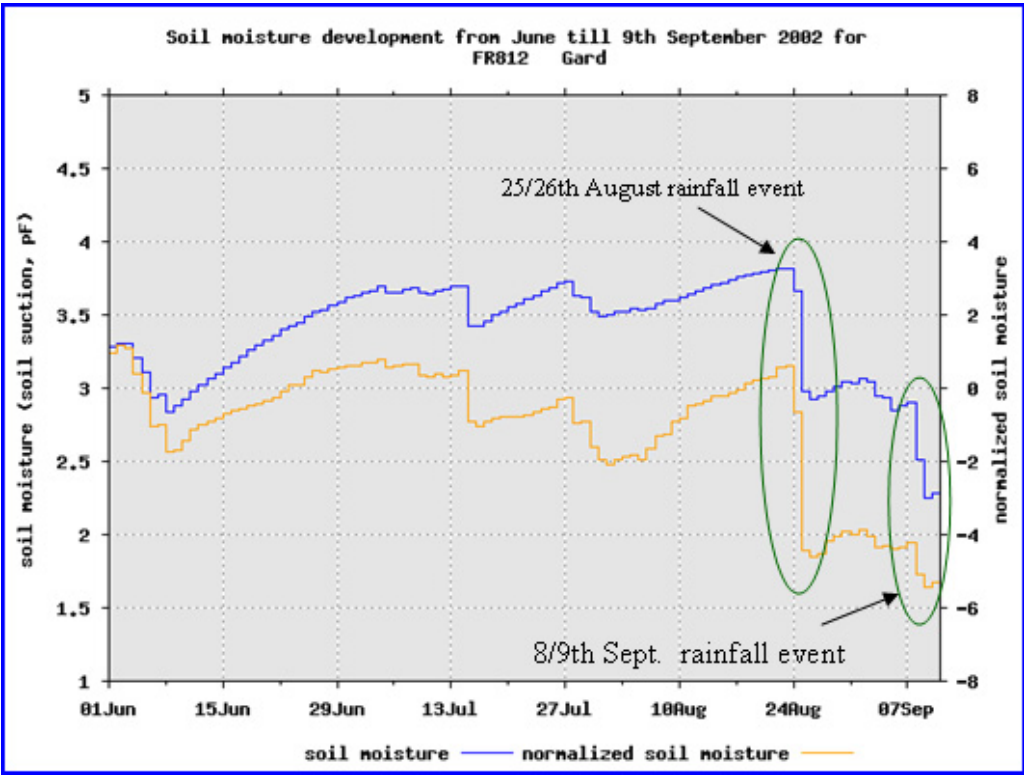


Fig. 3.1.5.4: Soil moisture development of Gard basin from 1<sup>st</sup> June 2002 to 9<sup>th</sup> September 2002.

Figure 3.1.5.5, shows the upstream daily rainfall for Gard at Corbes giving an idea about the rainfall amount from June to September 2002. It is clear that there was a 2-month dry period over the region till 25<sup>th</sup> August while intensive rainfall started on 26<sup>th</sup> which let the soil to be highly saturated with water. Although the total amount of rainfall on 26<sup>th</sup> August was higher than the amount of rainfall on 8<sup>th</sup>/9<sup>th</sup> September that generated the flash flood event, but the soil moisture conditions of the region was extremely dry before 26<sup>th</sup> August while on the contrary the soil moisture was extremely high before 9<sup>th</sup> September that facilitated the whole rainfall to be as an excess rainfall and later as surface runoff consequently the peak discharge was higher than the 26<sup>th</sup> – August peak discharge.

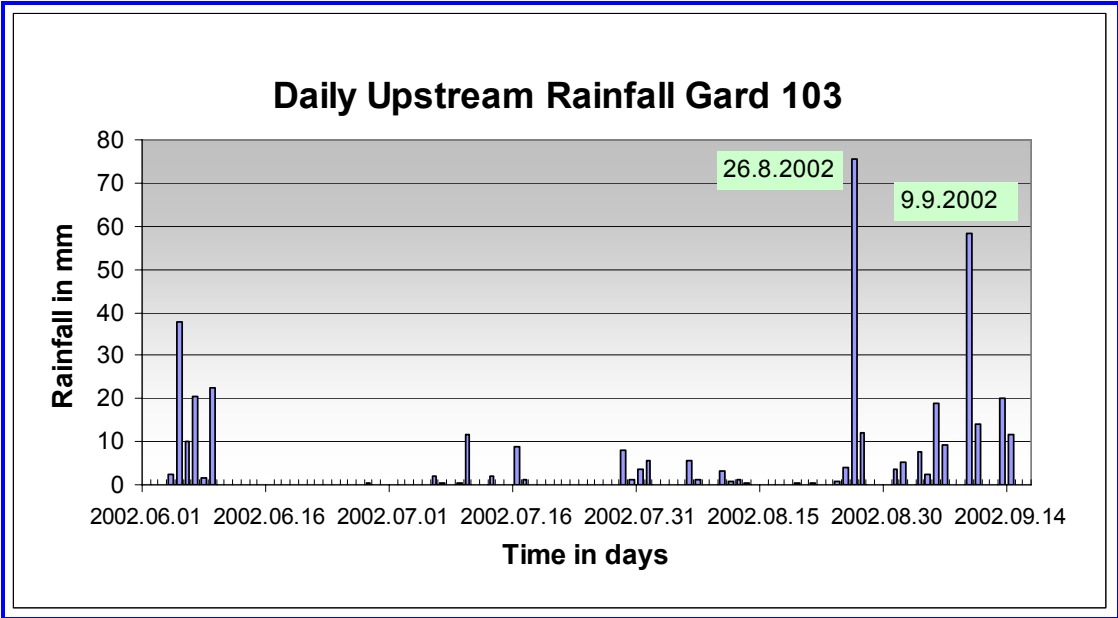


Figure 3.1.5.5, shows the daily upstream rainfall for Gard at Corbes

Table 5 shows the scheme how the results can be viewed in terms of threshold exceedance. In the left hand column the starting date of the flood forecasts is shown. The time intervals for which the flood warning information is evaluated is shown on the x-axis, top row. Each 48-hour forecast is split into 4 periods of 12 hours from 1-12 hours, 13-24 hours, 25-36 and 37-48 hours. During these 12-hour steps the highest flood alert level exceeded is color-coded within the table. The exceedance of the low, medium, high and severe thresholds is green, yellow, red and purple respectively.

The information from each forecast is shifted in a way that the time for which the forecasts are valid is aligned, e.g. the information for the 12 hour period from 9th September 00:00 to 12:00 are aligned in one column, and overlapping sections allow to see at one glance if the forecasts are persistent and consistent with the previous forecast.

This type of representation has been adopted from the visualization and decision rules of the European Flood Alert System (e.g. see Ramos et al., 2007). Persistent forecasts are treated with more confidence than non-persistent forecasts. Bartholmes et al. (2008) have shown that by taking into account persistence the number of false alarms decreases significantly.

Table 5 hereinafter shows which time steps correspond to the forecasting leadtime and dates. Overlapping periods between different forecasts are colour coded. For example the last 12-hours of forecast ALDWD200209071200: (AL37-48) overlap in time with the the 12-h time interval (AL25-36) of the subsequent forecast ALDWD200209080000.

Figure 3.1.5.6a to 3.1.5.6e show for each of the overlapping periods, the highest thresholds exceeded during each 12 hour interval, e.g. the highest threshold exceeded between time steps 1 to 12, 13-24, etc. The results are shown as maps and are colour coded according to the thresholds listed in Table 1.

Figure 3.1.5.6.a illustrates that no information could be drawn from the 20020907 00:00 forecast to indicate that a flashflood may take place. But already starting from the next forecasts at 20020907 12:00 (3.1.5.6.b) a clear indication of risk of flooding is present and also persistently forecasted in the subsequent forecasts. The results are equally consistent for the overlapping time periods.

Table 5: Temporal overlap of forecasted weather with 12-hours lead-time.

Forecasting Day and Time	To	0712	0800	0812	0900	0912	1000	1012	1100	1112	1200
AIDWD200209070000		AL1-12	AL13-24	AL25-36	AL37-48	Overlap	Overlap	Overlap	Overlap		
AIDWD200209071200			AL1-12	AL13-24	AL25-36	AL37-48	↓	↓	↓		
AIDWD200209080000				AL1-12	AL13-24	AL25-36	AL37-48	↓	↓		
AIDWD200209081200				↑	AL1-12	AL13-24	AL25-36	AL37-48	↓		
AIDWD200209090000				↑	↑	AL1-12	AL13-24	AL25-36	AL37-48		
AIDWD200209091200				↑	↑	↑	AL1-12	AL13-24	AL25-36	AL37-48	
AIDWD200209100000								AL1-12	AL13-24	AL25-36	AL37-48
			Overlap	Overlap	Overlap	Overlap	Overlap	Overlap	Overlap	Overlap	Overlap
AL1-12, AL13-24, AL25-36, AL37-48											
Maximum Alert during the period from first hour of forecasting to 12th hour and so on for the others											

The procedure has been carried out for calibrated and non-calibrated model and to show the reliability of flash flood forecasting particularly for 37-48 hours lead-time and for 25-36 hours as well.

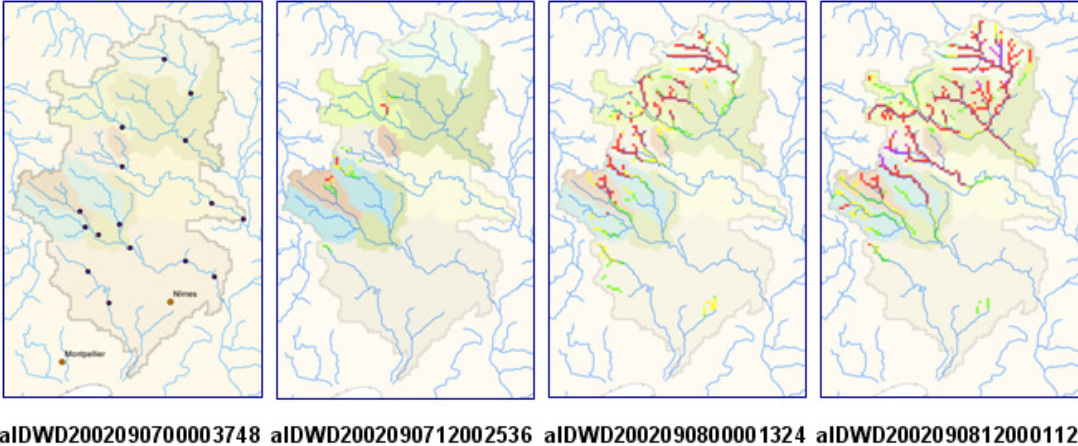
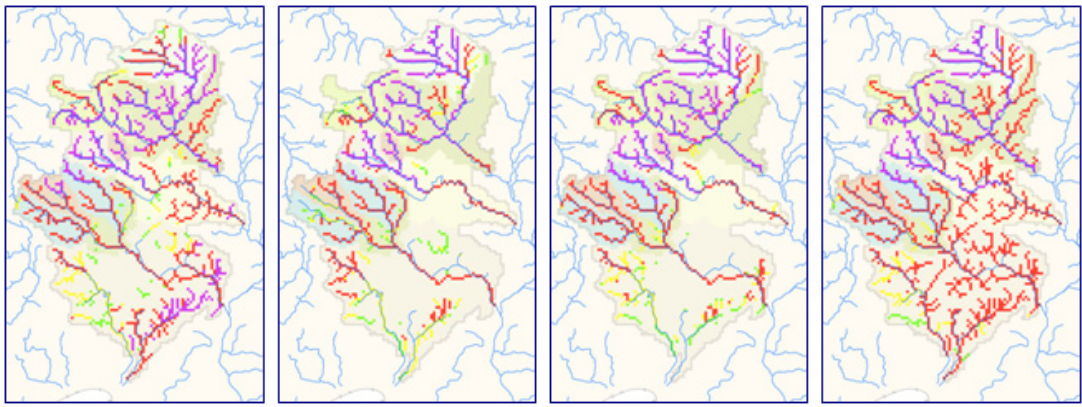


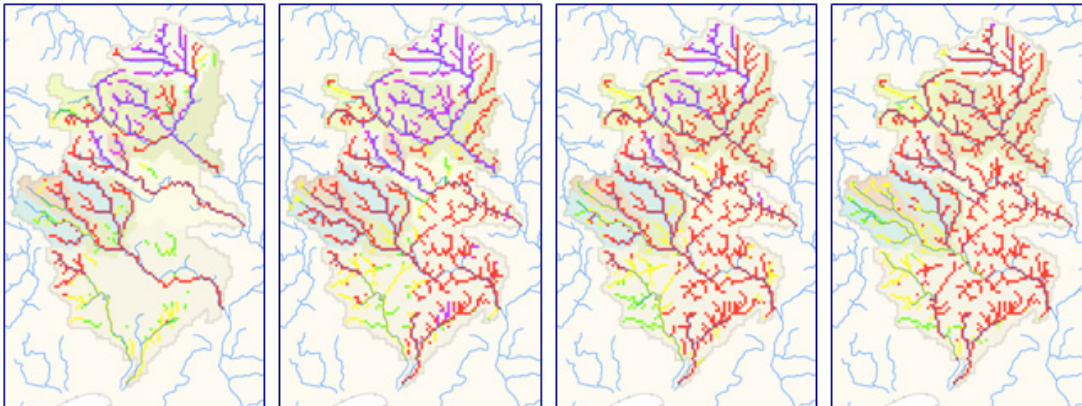
Figure 3.1.5.6a:





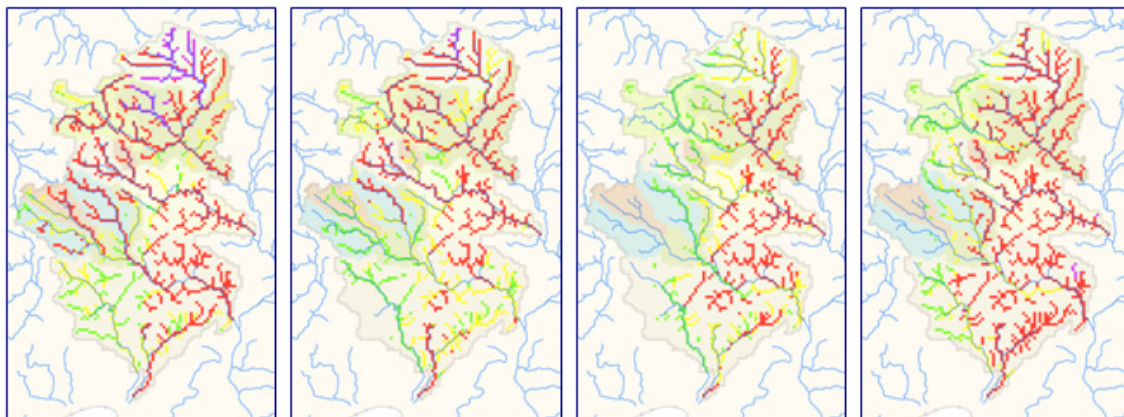
aIDWD2002090712003748 aIDWD2002090800002536 aIDWD2002090812001324 aIDWD2002090900000112

Figure 3.1.5.6b:



aIDWD2002090800003748 aIDWD2002090812002536 aIDWD2002090900001324 aIDWD2002090912000112

Figure 3.1.5.6c:



aIDWD2002090812003748 aIDWD2002090900002536 aIDWD2002090912001324 aIDWD2002091000000112

Figure 3.1.5.6d: legend



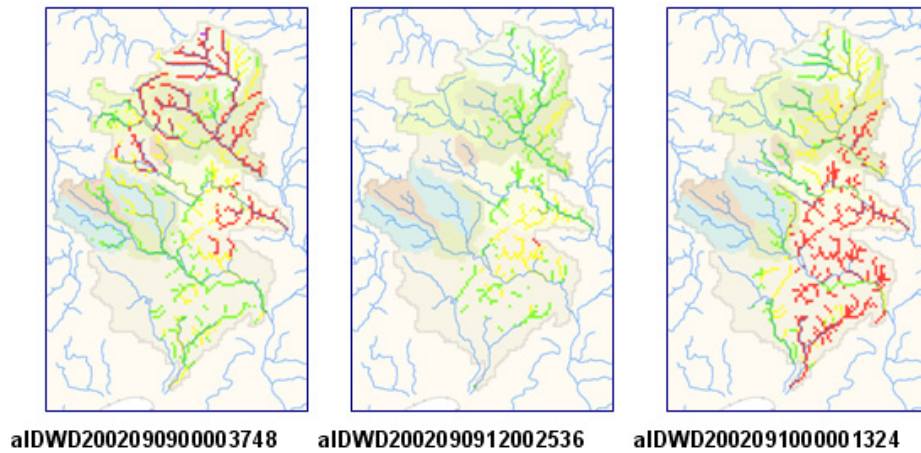


Figure 3.1.5.6e:

Figures 3.1.5.6 a-e: Spatial maps of highest thresholds exceeded during 12 hour intervals between overlapping time periods of successive forecasts Each 48-hour forecast is split into 4 periods of 12 hours from 1-12 hours, 13-24 hours, 25-36 and 37-48 hours.

In the end I would like to emphasize that in this case the reliability of deterministic weather forecasts driven by DWD is high for detecting this flash floods at least for the lead-time between 44-20 hours as shown in figure 3.1.5.7. This figure shows the spatial distribution of threshold exceedances for the event for three successive 12-hours lead-time forecast taking the 9th of September 2002 at 08:00 as a maximum observed peak discharge reached over the affected area.

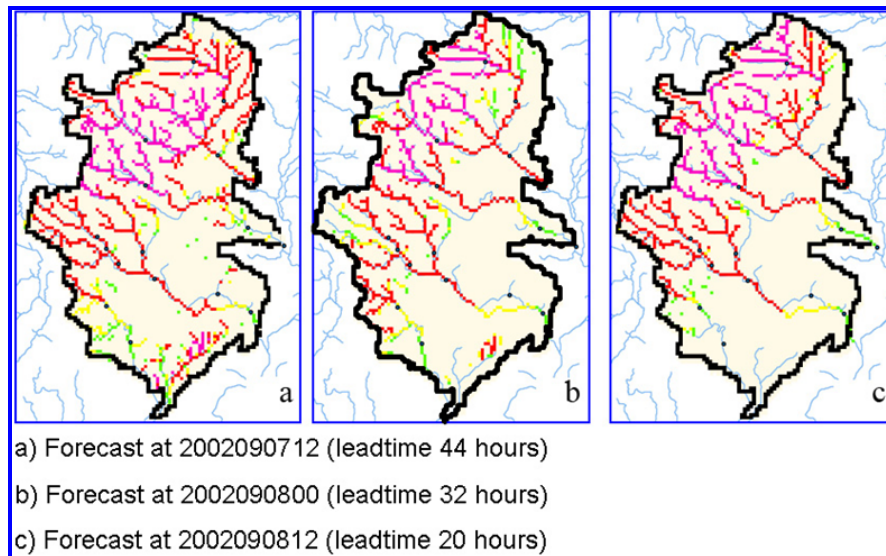


Figure3.1.5.7: Spatial distribution of threshold exceedances for the event for three successive 12-hours lead-time forecast as indicated in a, b, and c.

## 3.2. Flash flood event 29th August 2003 in river basins in Italy and Slovenia

### 3.2.1. The Fella River Basin of Eastern Italian Alps

The region considered in this case study (Figure 3.2.1.1) includes a portion of the central chain of eastern Alps and of the Alpine foreland region. The arc-shaped mountainous range of the eastern Alps constitutes the major topographic feature within the analysis domain. The most prominent valleys are aligned along the main ridge in the west-east direction for some tens of kilometers. The area is included within the Friuli-Venezia Giulia region, which borders to the north with Austria, to the east with Slovenia and to the west with Veneto. The region is characterized by three distinct pluviometric regimes: (i) the upper plain area, with mean annual precipitation (herewith called MAP) ranging from 1200 to 1500 mm; (ii) the Alpine foreland area, where MAP locally increases up to 3300 mm, which represents the highest mean values for the Alps; (iii) the inner Alpine area, where MAP decreases to 1600-1800 mm, due to rain shadow effect of the southern ridges (Borga, et al, 2007).

A description of the climatology of extreme subdaily rainfall is provided by the maps of the point average values of annual precipitation maxima (herewith called APM) for duration of 1, 3 and 6 h (Figure 3.2.1.2). The maps show clearly (i) the relatively high values of these rainfall accumulations, and (ii) the orographic control on the spatial distribution of the average values. It is interesting to note that the highest values for 6 h duration are located on the Alpine foreland area, while for 1 h duration high values are also found on the south-eastern coastal plain. The maps reveal also a marked decrease of the average APM values (for all durations) in the inner Alpine region.

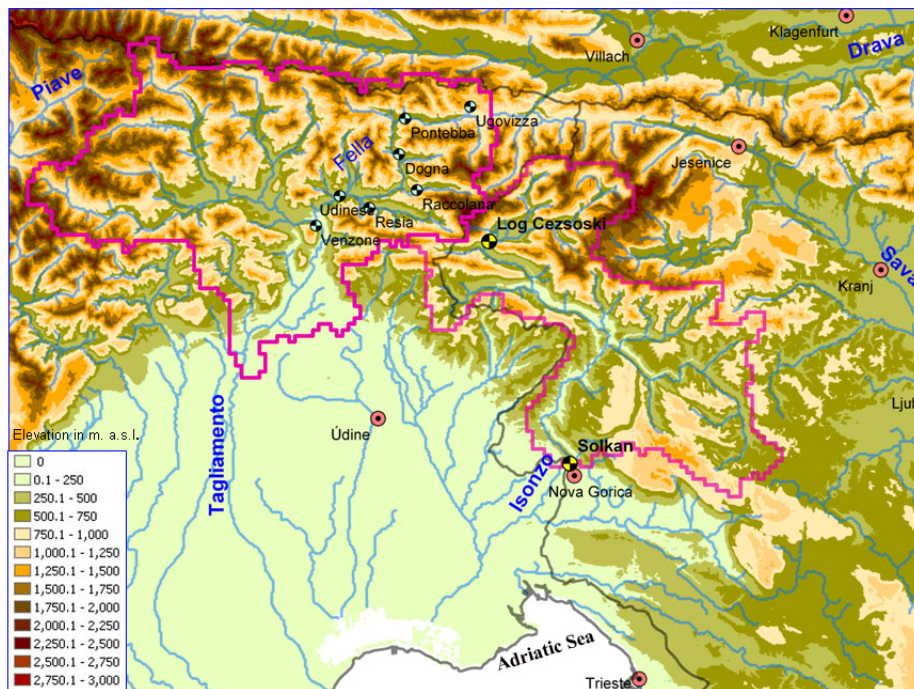


Figure 3.2.1.1: Topography of the study area, eastern Alps and of the Alpine foreland region, with the catchments used for this study.

The Tagliamento River is a braided river and the dominant river system in the region flowing from the Alps to the Adriatic Sea at a point between Trieste and Venice. The watershed covers an area of 2,916 km<sup>2</sup>. From north to south (a linear distance of <100 km), the Tagliamento traverses four major regions: (i) the Julian and Carnian Alps, (ii) Alpine foreland area, (iii) the upper and lower Friulian plain, and (iv) the coast (Figure 3.2.1). The alpine area of Friuli mainly consists of limestone, with a spatial sequence of Silurian, Devonian, Triassic, Jurassic and Cretaceous formations north to south (Astori, 1993; Martinis, 1993; Cucchi et al., 2000). Some portions of the regions are characterised by karstified limestone. The catchment is tectonically active, continuously developing faults and overthrusts. Many tributary streams, like the Fella, have sharp bends following the direction of these faults (Figure 3.2.1.3). The pre-alpine mountains mainly consist of limestone (Jurassic-Cenozoic) and Flysch (calcareous flysch, molasse) (Ward et al., 1999).

The Tagliamento is characterized by a flashy pluvio-nival flow regime, with the highest average discharges in spring (snowmelt runoff) and autumn (rainy period). At Pioverno (catchment area around 1866 km<sup>2</sup>) the average annual precipitation amounts to 2150 mm and average discharge is 91m<sup>3</sup>s<sup>-1</sup>. The August 2003 flood focused on the 705 km<sup>2</sup>-wide Fella basin (Figure 3.2.1.1), which is a major left-hand tributary of the Tagliamento river system. This basin has a mean altitude of 1140m.

From a geomorphological and hydrogeological prospective this plain is subdivided in two provinces which are separated by a resurgent line. The Upper Friuli Plain is mostly composed of calcareous and dolomitic gravels and hosts a well developed phreatic aquifer. The Lower Friuli Plain is characterized by multi-layered artesian aquifers that are composed of gravels and sand interbedded by clay and silty layers that become thicker in a southwards direction (Cucchi, et al, 2000)

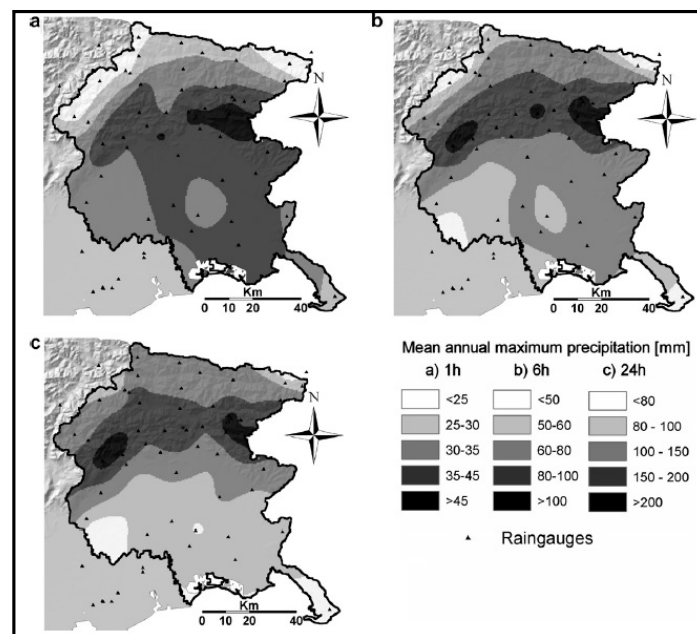


Fig. 3.2.1.2 a, b, c: Maps of point average of maximum yearly rainfall for durations of (a) 1 hours, (b) 3 hours, and (c) 6 hours, for the Friuli region. Triangles represent the position of the stations used to draw the maps (Borga, et al, 2007).

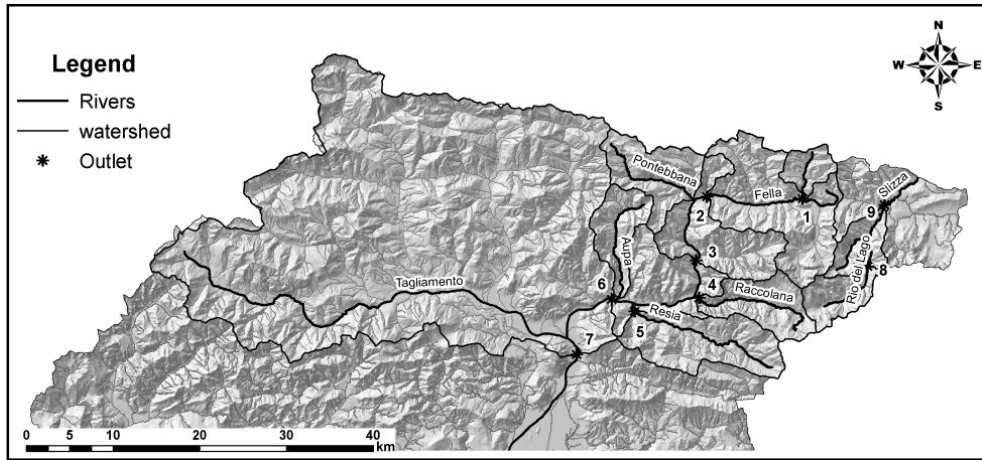


Figure 3.2.1.3: Catchment map of the upper Tagliamento river basin, with subcatchments of the Fella river basin. (1): Uqua at Ugovizza; (2) Fella at Pontebba; (3) Fella at Dogna; (4) Raccolana at Raccolana; (5) Resia at Borgo Povici; (6) Fella at Moggio Udinese; (7) Tagliamento at Venzone; (8) Rio del Lago at Cave del Predil; (9) Slizza at Tarvisio (Borga, et al., 2007).



### 3.2.2. The Soca (Isonzo) River Basin

The river Isonzo, in Slovenia known as the Soča, has its source in Slovenia and empties into the Adriatic Sea. So that Slovenia (upstream country) and Italy (downstream country) share the Isonzo basin Figure 3.2.2.1. The basin has a pronounced mountainous character with an average elevation of about 599 m above sea level. Major trans-boundary tributaries include the rivers Natisone, Vipocacco and Iudrio.

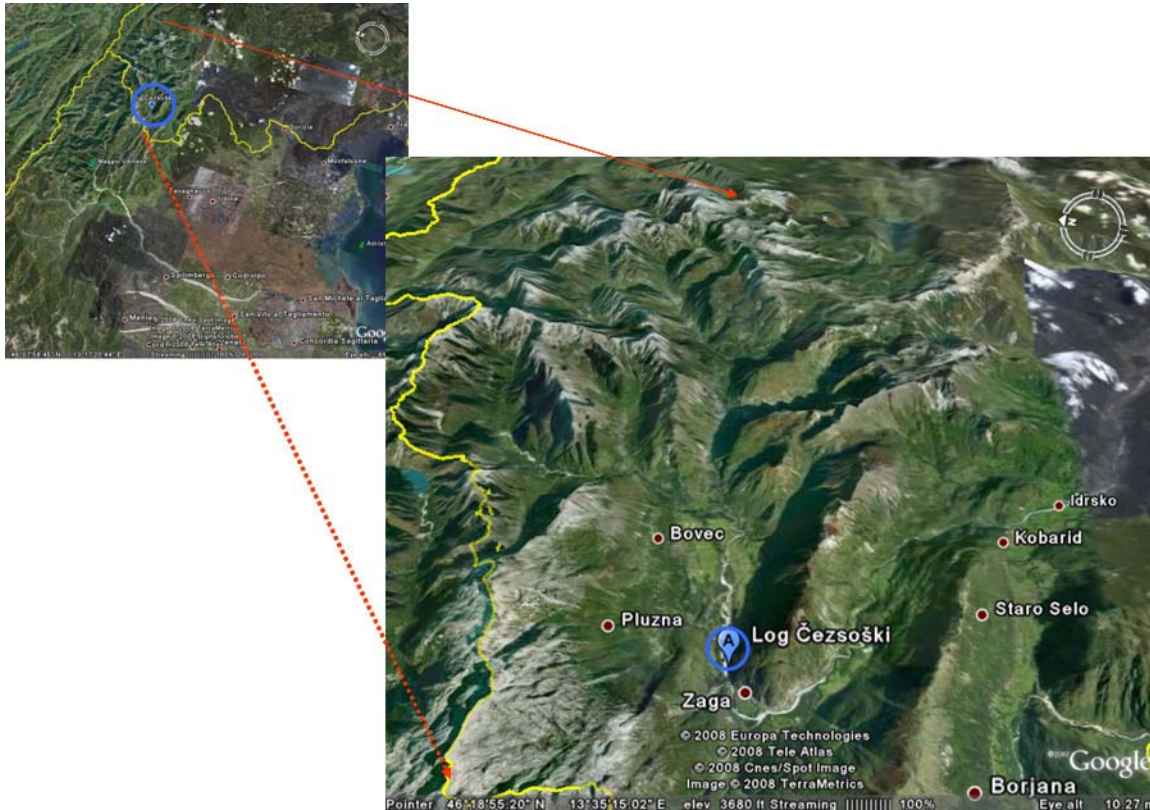


Figure 3.2.2.1: Topography of the upstream part of Isonzo River Basin in Slovenia showing the steep sloop mountainous landscape.

As shown in Figure 3.2.2.2 the major floods during the last 6 decades were occurred during autumn season between September and November.

### Flood Events Above Observed High Threshold for Isonzo river at LogCezsosik from 1948 to 2004

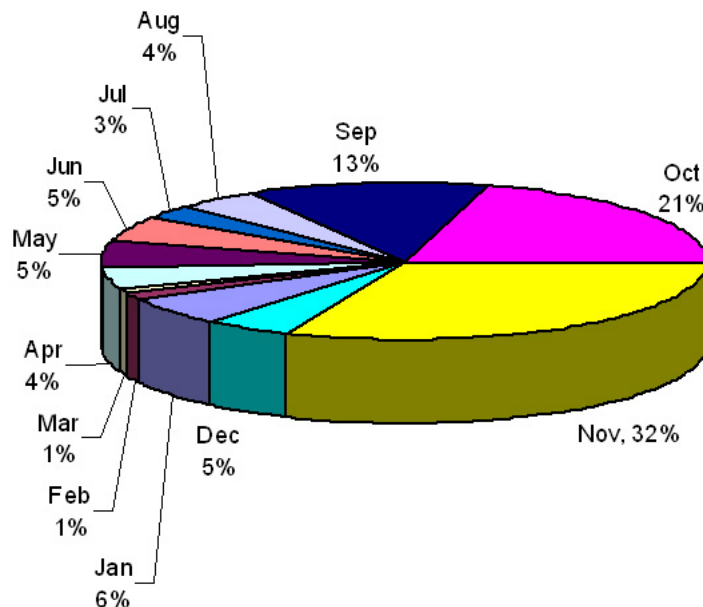


Figure 3.2.2.2: Distribution of observed flood events over the months for the Isonzo River at Log Cezsosilk stream gauging station from 1948 to 2004.

#### 3.2.3. Description of the 29th August 2003 case study

The area under study is characterized by frequent heavy precipitation. Daily rainfall amounts exceeding 500 mm may be locally recorded in this area in a 20 to 30 years time span (Villi et al., 1986; Ceschia et al., 1991). During late fall, winter and spring, heavy precipitations are normally related to synoptic circulations and to southerly humid flows. During summer and partially during fall, the contribution from convective or mesoscale rainfall becomes significant or even prevailing. Due to the rugged topography of the region, together with its densely fractured bedrock and its high seismicity (Querini, 1977), heavy convective precipitations result often in flash floods, associated to diffused land sliding, debris flows and sediment transport.

The exceptionally hot June and the long term average significantly warmer July, has followed the extremely hot in August and rounded up by far the warmest summer ever. With few exceptions, August 2003 was so far warmer than the warmest month with we ever had, this is August 1992; in a large number of stations was also the highest ever measured air temperature. In most of the country was extremely severe drought in August at above-average sunny and hot weather and the absence of rainfall escalating. Despite the extreme heat storms were also common, although few storms were accompanied by a strong local wind and hail and cause damage. Extremely heavy rainfall last days of August have caused problems in Zgornjesavski valley. Due hudourniških coatings grušča and sludge to the ground and landslides have been for some time, disconnected from all road links with Zgornjesavsko valley. Last August, while the penetration of cold air announced, at sea,

strong Tramontana surprised many sailors and done much damage; along the coast were also victims of the death.

On 29<sup>th</sup> August 2003, at the end of a prolonged drought, a large atmospheric disturbance interested a wide area in the Central and Eastern Alps, from the Tessin Valley (Switzerland) to Lower Carinthia in Austria. A Meso Scale Convective System affected the study area, starting at 10:00 LST and lasting for approximately 12 hours. Prior to the development of convection, the atmosphere was characterized by strong instability as evidenced by the very high CAPE value on the Udine radio sounding of 29 August 2003 at 06:00 UTC (about 4000 J kg<sup>-1</sup> for the CAPE computed based on the most unstable parcel. Precipitated water computed for these radio-sounding amounts to 44mm and shows that the humidity content of the atmosphere was already high. The storm affected a 1,500 km<sup>2</sup> wide area, and caused loss of lives and substantial disruption of the local economy, with damages close to 1 billion Euros (Tropeano et al., 2004).

The 29<sup>th</sup> August 2003 flood is also of particular interest because it provides an end member in the spectrum of impacts of antecedent soil moisture on extreme floods (Borga, et al, 2007). The event resulted indeed as a combination of two extreme events, since very large accumulations of rainfall over 3-6 hours occurred at the end of a climatic anomaly of prolonged drought and warm conditions in Europe and over the Mediterranean. Analysis of temperature records over Europe shows that the 3 months period June–August 2003 has been probably the warmest since 1500 over Western Europe (Casty et al., 2005). The drought culminated in August, but precipitation accumulations were below average since the beginning of the year. At the Udine rain gauge station, close to the study area, the cumulative precipitation total for the first eight months of 2003 was around 50% of the climatological average. These conditions brought to very low soil humidity at the beginning of the event. A heavy localized thunderstorm which occurred the day before the flood on a portion of the Fella river system introduced elements of spatial variability in the pattern of soil moisture initial conditions.

Whereas it is generally recognized that antecedent soil moisture is of little importance in determining the magnitude of extreme floods (Wood et al., 1990), the August 2003 flood provides a counter example of the possible role of low antecedent soil moisture conditions, when combined with high soil moisture capacity, on reducing the flood response of extreme storms. Large initial losses and non-linearities related to the wetting-up processes and to the extension of the river network to unchannelised topographic elements are examined in this study. These non-linearities and the concentration of rainfall on quasi-stationary convective bands provided a dominant control on scale-dependent flood response in watersheds of the upper Tagliamento river basin (Borga, et al, 2007).

Figure 3.2.3.1 shows the soil moisture conditions of the study area expressed in pF value before and after the flood event which gives an idea about the soil moisture content and the degree of scarcity of water in the soil. High pF means low moisture content and vice versa. In addition, this figure shows that before the flood event the pF value was about 3.7 in both Tagliamento and Isonzo watersheds while pF value after the event was about 3.4. The soil moisture and the 12-years daily average values of the soil moisture simulated by the model for the upstream area of each selected outlet point for July, August and September are shown in Figure 3.2.3.2. The runoff response was rapid, despite dominantly forest cover, due to thin soils, steep slopes (mountainous region) Figure 3.2.2.1. Therefore the role of antecedent moisture in flood response in this flash flood event can be negligible.

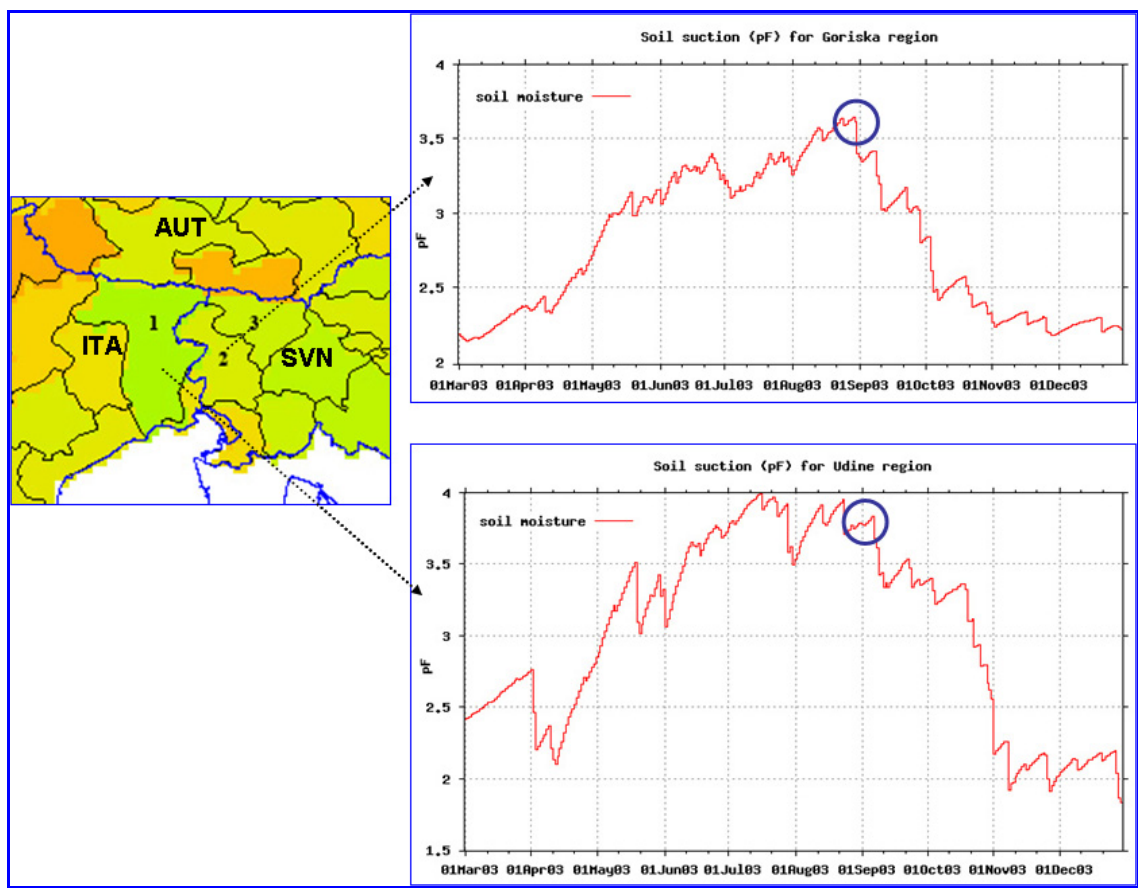


Figure 3.2.3.1: Shows the pF value in the region before and after the flood event



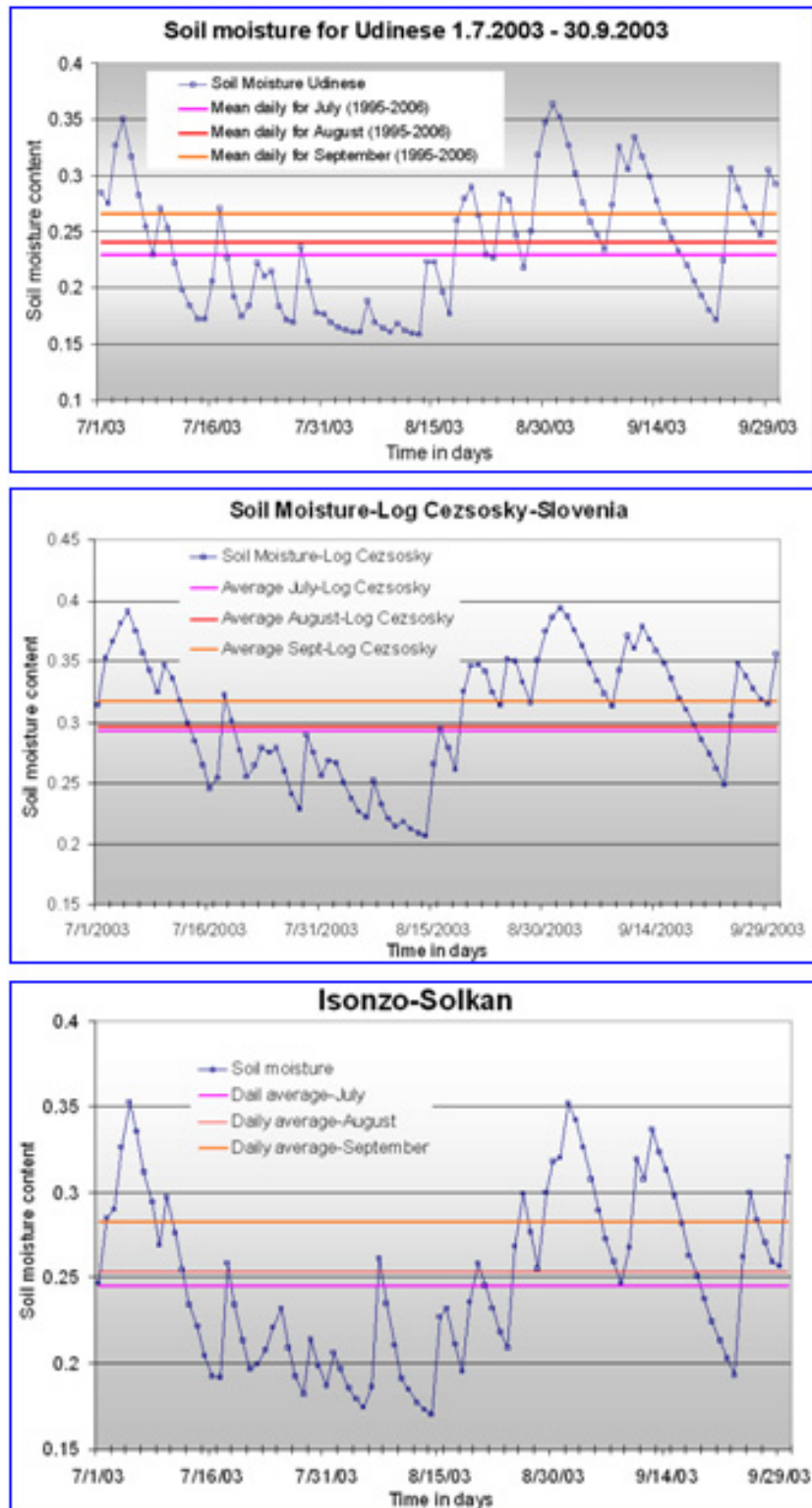


Figure 3.2.3.2: Shows the soil moisture contents upstream of each stream gauging station. The simulated daily average soil moisture for July, August and September for long-term simulation, from 1995 to 2006, has been plotted as well.

### 3.2.4. Input data for the two studies

For the determination of the hydrological regime over the past years, synoptic meteorological station data from the data archive of the AgriFish<sup>ii</sup> unit at the DG Joint Research Centre have been used. Their database holds reliable meteorological data from about 2000 stations across Europe since 1990. In the study area few meteorological stations are available for which daily values of temperature and rainfall have been reported and potential evaporation estimated. These data have been used to calculate the water balance and the initial conditions for running the model for the forecasting periods.

The missing of long-term observed discharge data of all stream gauging stations in the study area was the reason for skipping the long-term simulation study comparable with the observed discharge. The estimated discharge data for the flood period have been used for comparing with the forecasted ones.

High-resolution operational weather forecasting data are provided to the JRC for research by the German national weather service (DWD). In 2002 the Lokalmodell of the DWD had a grid spacing of 7km, an hourly temporal resolution, and a forecasting lead time of 48h. The DWD forecasts are provided every 12 hours starting at 00UTC and 12UTC.

Figure 3.2.4.1: shows the rainfall amount causing the flood event in Upper Isonzo.

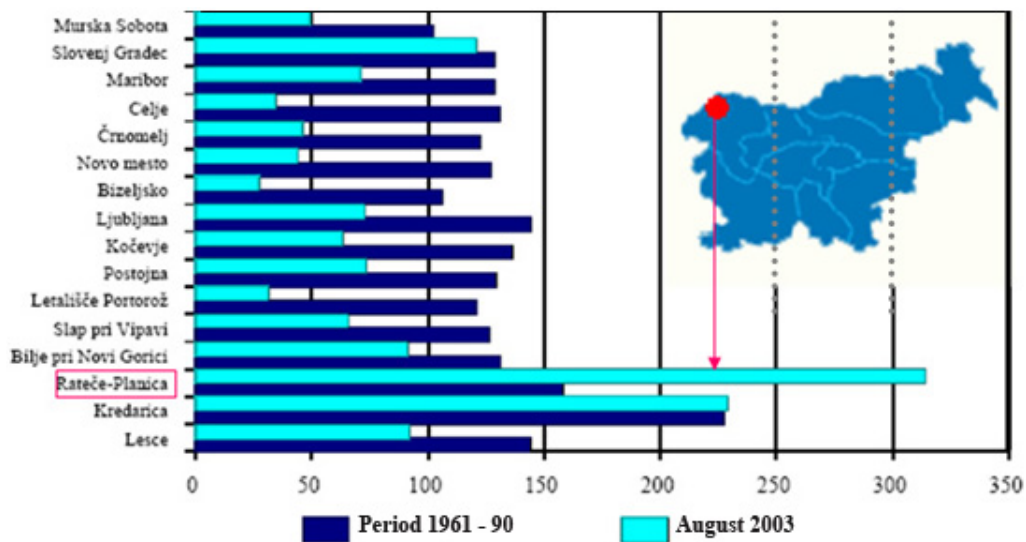


Figure 3.2.4.1: Monthly precipitation amount in August 2003 and the 1961.1990 normals (after Slovenian Monthly Bulletin, Ljubljana, August 2003, Number 8)

### 3.2.5. Results

The hydrological regime of the Fella and Isonzo river basins is illustrated in (Fig. 3.2.1.1). Despite the coarse meteorological station network data used as input, the simulations capture the periods of high flows reasonably well. Although peaks are both over- or underestimated, the model rather tends to underestimate the discharges particularly severe alert levels.

Figure 3.2.5.1 shows the spatial distribution of threshold exceedances, i.e. highest threshold exceeded during forecasting period. In this figure, a signal of having flash flood was detected on 27<sup>th</sup> August 2008 at 12 o'clock forecast run, that means more than 48 hours from the peak time in the most downstream at Udinese stream gauging station.

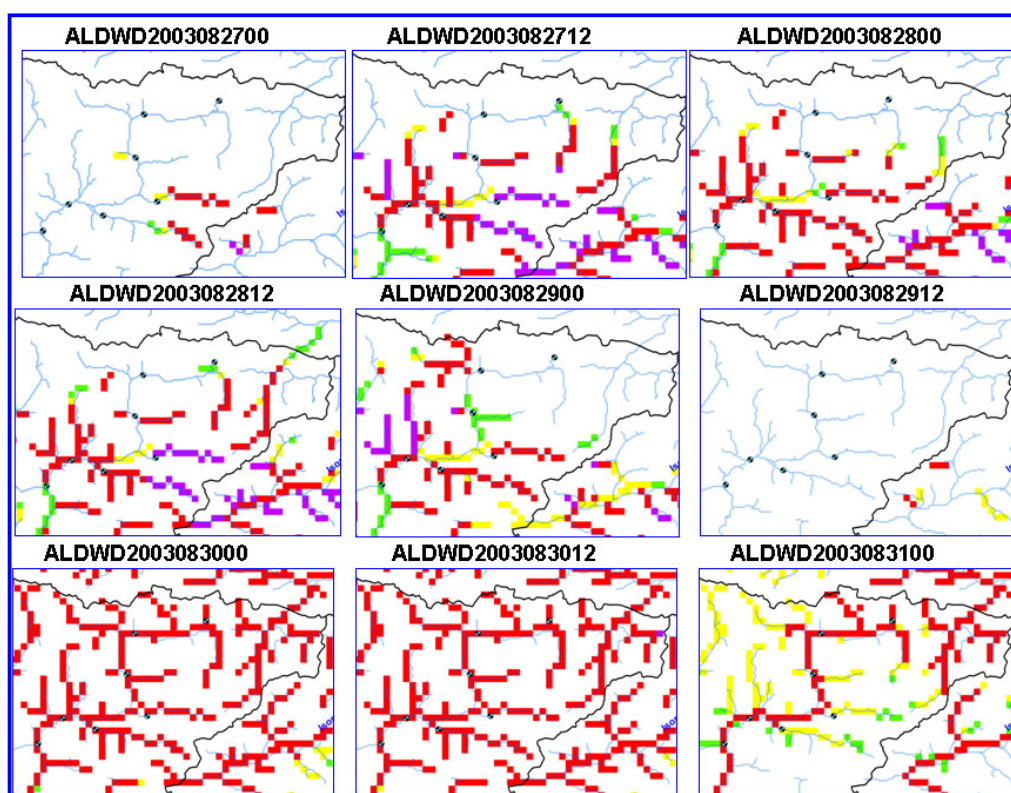


Figure 3.2.5.1: Summary threshold exceedance maps showing the highest threshold exceeded during the 48 h forecasting time for flood forecasts based on the DWD Lokallmodell weather forecasts from 20030827 00:00 and in 12 hourly steps until 20080831 12:00. The threshold exceedances are color coded with purple (severe), red (high), yellow (medium) and green (low).

Figures 3.2.5.2, 3.2.5.3, and 3.2.5.4 show the hydrographs of observed hourly discharge against the forecasted discharges for two gauging stations in Fella watershed and one in Upper Isonzo watershed in Slovenia.

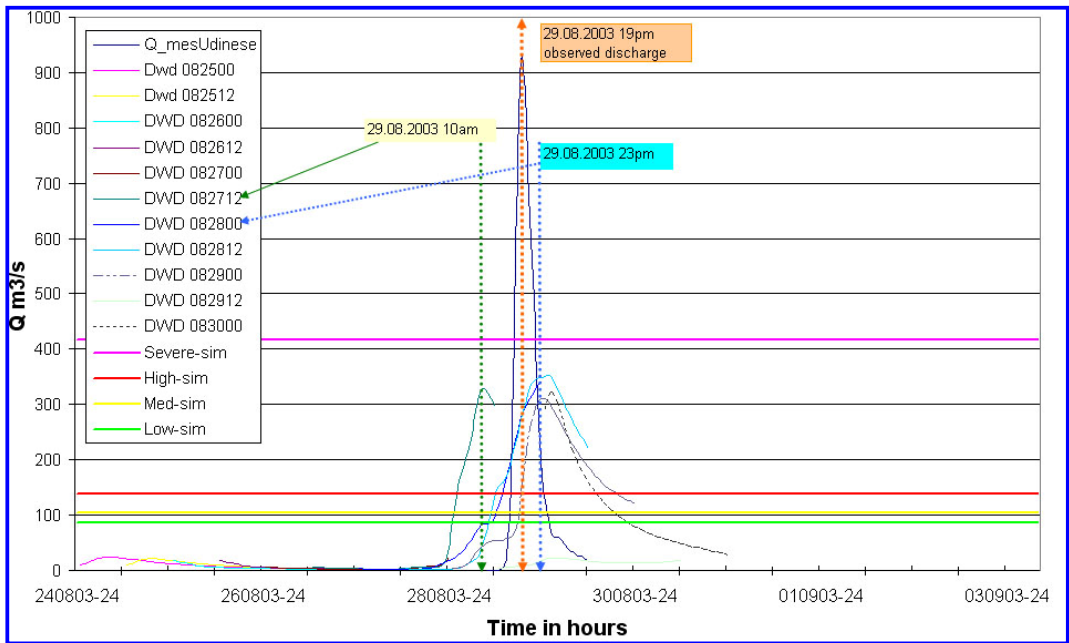


Fig. 3.2.5.2: a- Observed hydrograph at Udinese in the Fella River with the vertical line indicating the time of peak at 19:00 on 29th August 2003. Hydrographs of forecasted discharges in m³/s (y-axis) for Udinese (623km²) in the Fella River from the 25th-30th Aug 2003 starting at 00:00 in hourly time steps (x-axis). The exceeded thresholds are color coded as purple (severe), red (high), yellow (medium) and green (low).

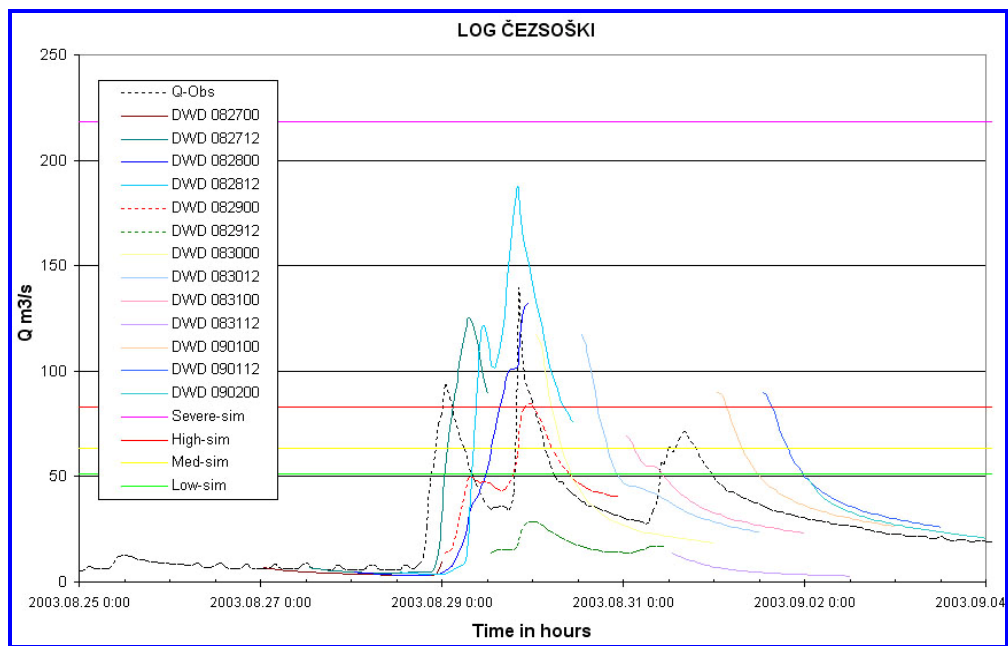


Fig. 3.2.5.3: Observed hydrograph for Fella River at Racollana gauging station.

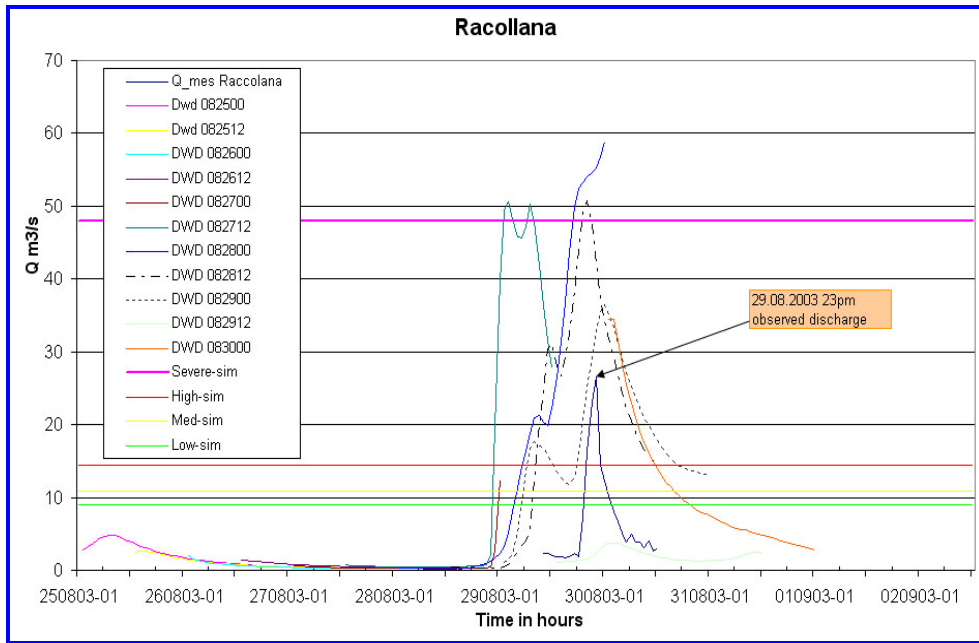


Fig. 3.2.5.4: Observed hydrograph for Isonzo River at Log Cezsoski gauging station.



### 3.3. The flash flood event 24th October 2006 – Slovenia

#### 3.3.1. The Goriska Region North-West part of Slovenia

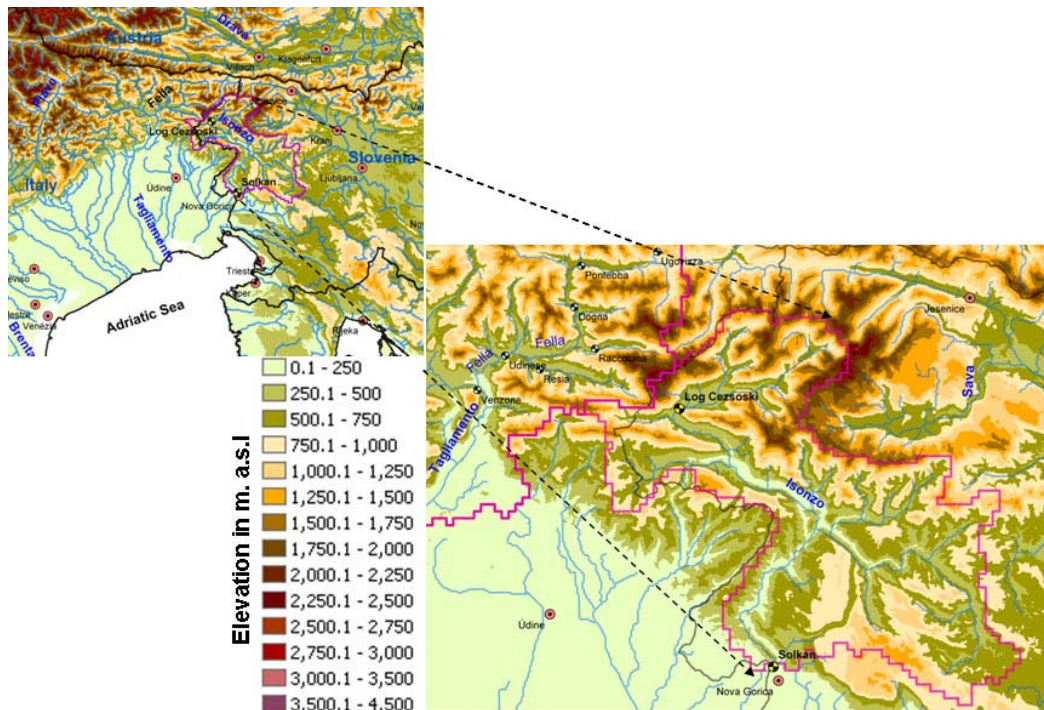


Figure 3.3.1.1: Map showing the study area.

The Soca River basin is in its upper part a typical glacial valley with steep gradient tributaries, and is situated along the Slovenian-Italian border. With an average annual precipitation of over 3000mm, and locally of nearly 4000mm, it is one of the wettest places in the Eastern Alps. Due to the prevailing sub-Mediterranean climate in the region and its location near the Po River plain and the Genoa area of low pressure, it is known to be hit by more than 40 thunderstorms a year on average, as shown by Brilly et al. (2000). Throughout history, local residents have accommodated to such wet climate and frequent flash floods, Mikos M., et al (2004).

### 3.3.2. Description of the 24th October 2006 case study

On 23<sup>rd</sup> / 24<sup>th</sup> October 2006 a sudden and unexpected heavy precipitation event was responsible for causing a flash flood in north-western part of Slovenia, particularly the upstream part of Soca (Isonzo) river basin, Figure 3.3.2.1 shows the observed rainfall caused the flood event.

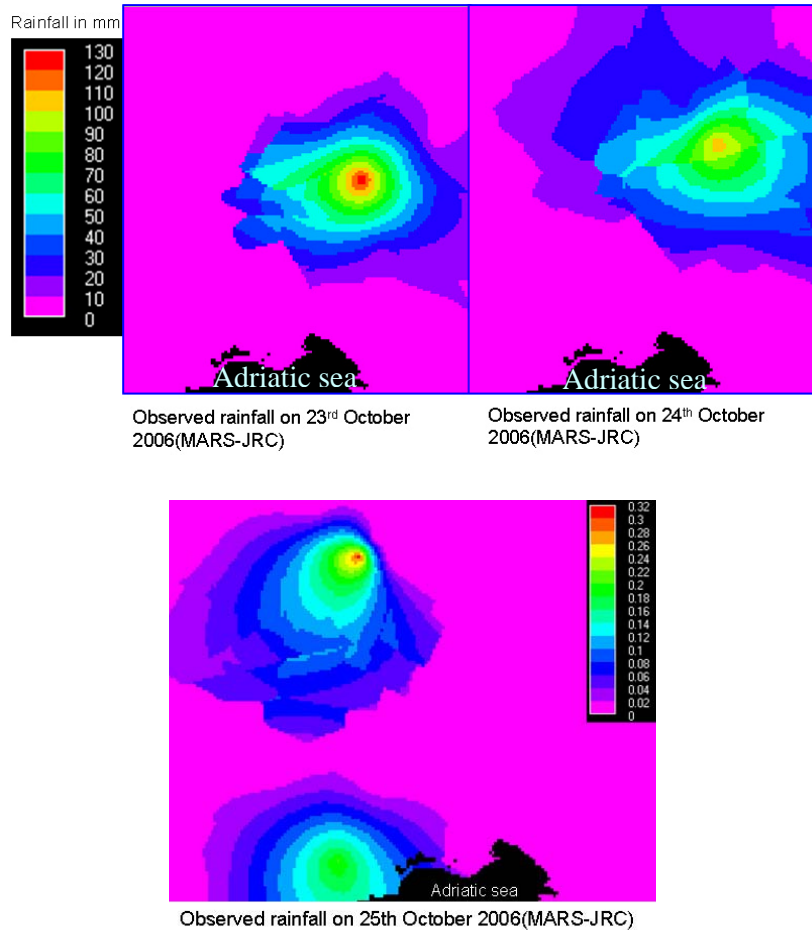


Figure 3.3.2.1: Observed daily accumulated rainfall from 23<sup>rd</sup> to 25<sup>th</sup> October 2006.

The event started just before the midnight of 23<sup>rd</sup> October and continued till the morning of 24<sup>th</sup> October which lasted for about 8-9 hours. This might be due to convective cells forming over the Adriatic Sea. The convection progressed northward to form inland a mesoscale convective system over this region. The quasi-stationary system stayed over the same region until approximately the next morning. This was diminished westward.

Input data for this event study are the same as mentioned in 3.2.4 with different time-related inputs. The forecasted rainfall data from DWD are shown in the figure 3.3.2.2 below:



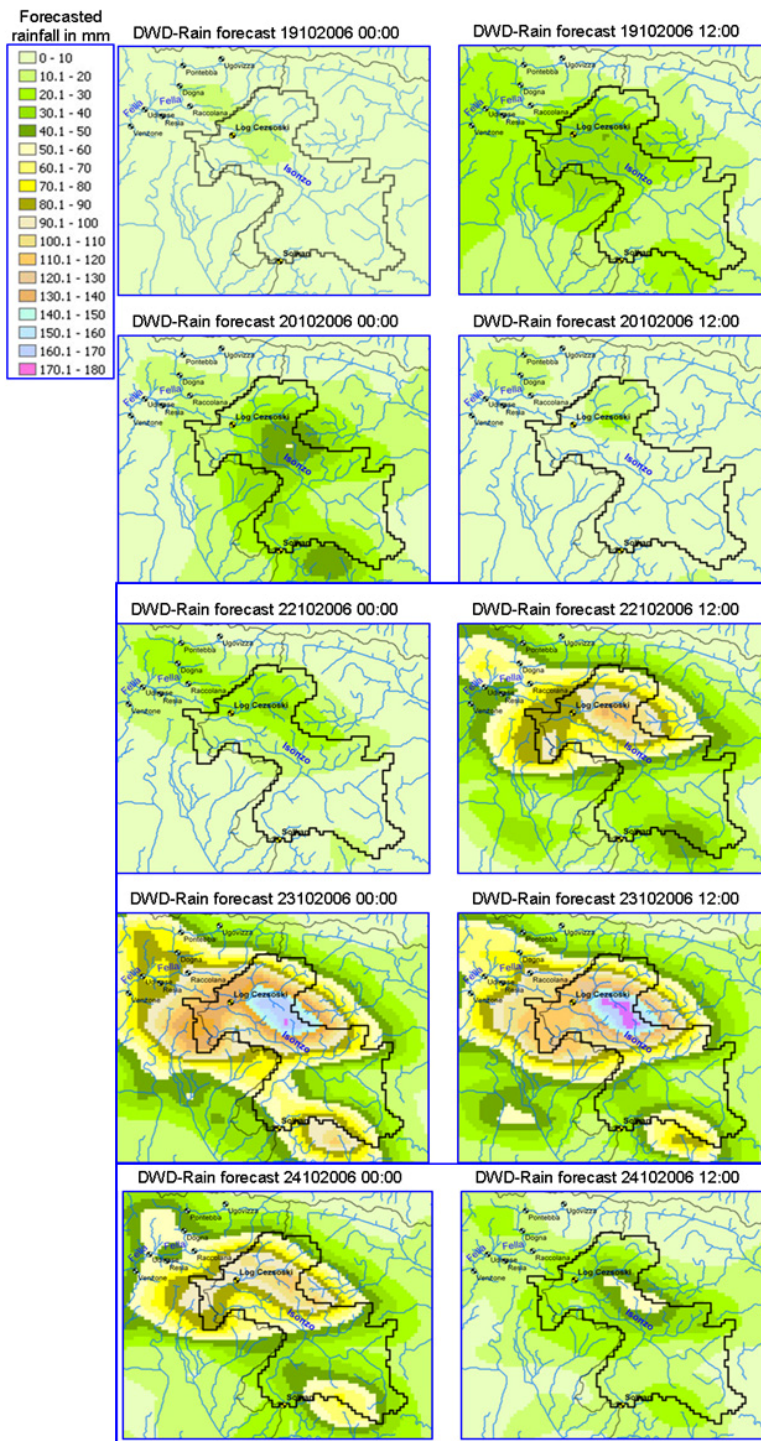


Figure 3.3.2.2: Accumulated 12-hours lead-time forecasted rainfalls from the 20061019 00:00 to 20061024 12:00.

### 3.3.3. Results

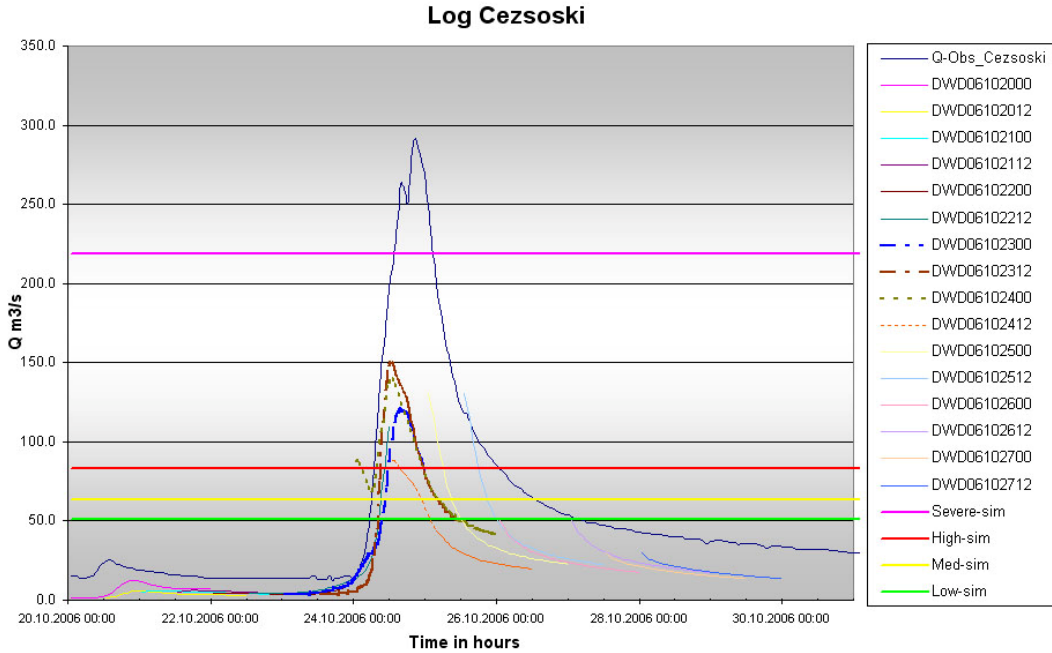


Figure 3.3.3.1: Comparing observed discharge from 1km grid resolution for Log Cezsoski with the forecasted discharge giving underestimation of the resulting discharge, while with the model consistent threshold; the high threshold is reached with the forecast from 22nd October 12:00 onwards.

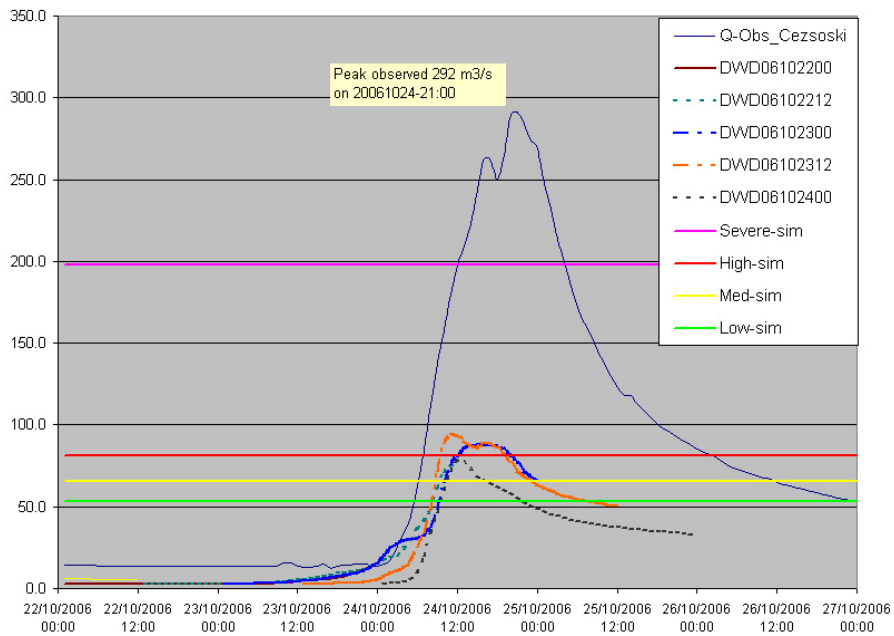


Figure 3.3.3.2: Comparing observed discharge from 5km grid resolution for Log Cezsoski with the forecasted discharge giving underestimation of the resulting discharge, while with the model consistent threshold; the high threshold is reached with the forecast from 23rd October 00:00 onwards.

Comparing the results from 1x1 km<sup>2</sup> grid resolution with 5x5 km<sup>2</sup>, it is clear that with the 5km grid resolution the DWD06102212 12:00 is not exceeding the high threshold while it does with the 1km grid. (Compare also the results from figure 3.3.3.1 with figure 3.3.3.2). This is not a surprising result since the 1km grid is more suitable to resolve the small scale processes playing a major role for flashfloods. Probably the grid spacing should even be higher. The threshold exceedance maps are shown in figure 3.3.3.3.

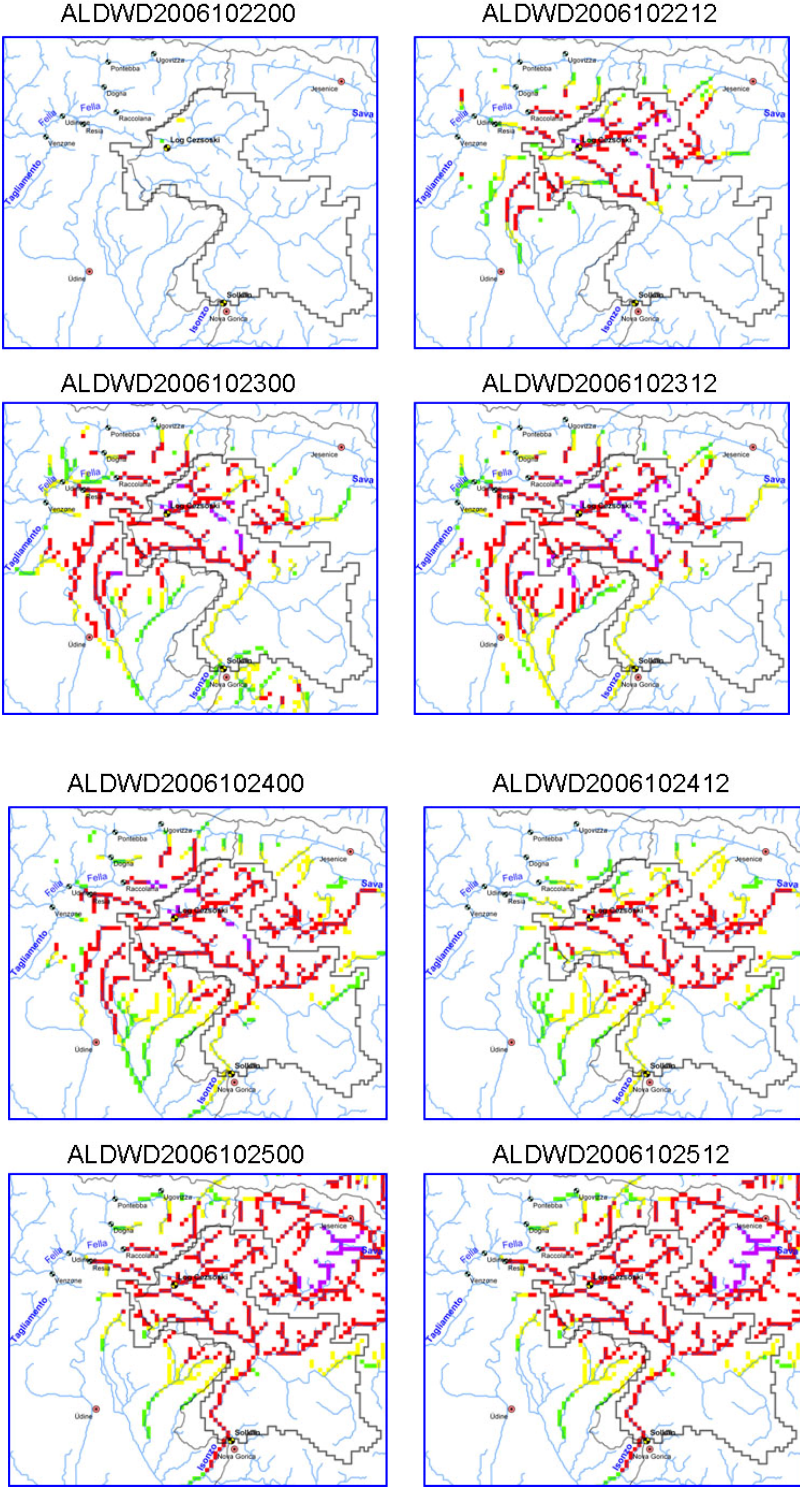


Figure 3.3.3.3: Flood threshold exceedance maps with 1km grid resolution for the Isonza catchment.



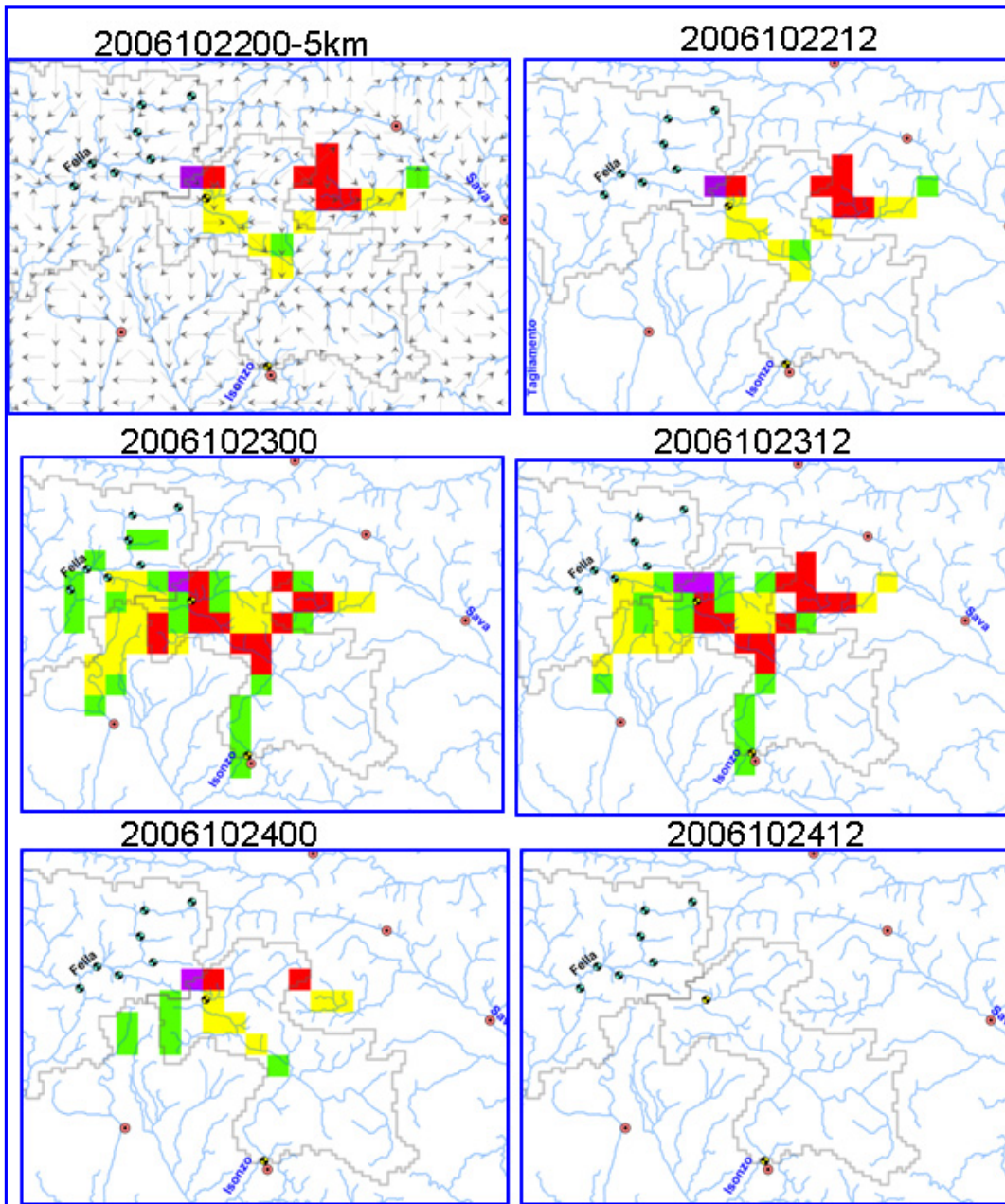


Figure 3.3.3.4: Spatial distribution of flood threshold exceedances, i.e. highest threshold exceeded during forecasting period for Slovenian part of Isonzo river basin with 5km grid resolution.

## 4. Summary and Conclusions

In this report the feasibility of interfacing short-range numerical weather forecasts with a spatially distributed rainfall-runoff model for early flash flood warning in ungauged river basins has been explored for several case studies. The methodology is based on flood threshold exceedance approach that was first postulated for the European Flood Alert System (EFAS) where the thresholds are derived from long-term simulations with an essentially uncalibrated hydrological model. The same model is then used with weather forecast data and the model-consistent thresholds applied for the analysis.

The proposed forecasting strategy addresses a number of shortcomings typically present in flash flood forecasting, namely coarse meteorological station networks and few or no discharge station data. Further, the advantage of using a distributed hydrological model together with this approach is that conditions of the soil, e.g. antecedent soil moisture, are directly calculated by the model and do not need to be estimated through other means. The study has shown that the the initial soil moisture condition plays a vital role for the generation of the flash flood event.

Results of the study show that by looking at relative differences and model-consistent thresholds, early warning for flash floods can be given with lead-times exceeding 24 hours. In the case of the 8-9th September 2002 event, the weather forecasts together with threshold exceedance method enabled the timing and severity of the event to be captured with an absolute lead-time of more than 36 hours. In terms of spatio-temporal distribution the event was forecasted too far north, leaving the Gard river basin only with high and not severe threshold values exceeded. Taking into account computing time, processing time and analysis time, the effective lead-time could still have been in the order of 24 hours. A six-month analysis confirms that the approach is capable of capturing major events. However, due to the more widely spread forecasted rainfalls; the number of false alarms is relatively high. Therefore the results of such an early warning system should only be used by local flood forecasters as a first indication that a severe event might take place, and should not be distributed to the public.

The number of misses, on the other hand, is comparatively low. This is important since missed events in terms of early warning are more important than false alarms, which can be easily identified in the subsequent hours. In the case of a missed event, however, the benefit of early preparedness measures is lost.

Due to the high uncertainty in heavy precipitation forecast the next step would be to explore these simulations with high resolution ensemble prediction system forecasts rather than deterministic forecasts. This would imply, however, a high computational burden. One possibility would be to simulate the hydrological processes on a coarser grid, e.g. 5km, and then zoom onto a higher grid resolution in case the coarser grid indicates a possibility of flooding. This is proposed to be explored during an upcoming research project called IMPRINTS. Tests with different grid resolutions have been performed for this study, e.g. between 5 and 1km grid spacings, which indicate that although the higher resolutions yield better results, simulations on 5km can be informative. Relying entirely on coarse simulations does, however, not seem to be feasible.

A first attempt of combined analysis of the physical and human responses to this devastating Mediterranean storm (Ruin et al., 2007) shows that most of the casualties were not prepared

for (1) the strength of the event and its consequences in terms of water speed, and (2) the time evolution of the storms. In 2002, the warning system, mainly based on the meteorological forecasts, was not designed to give a hydrological signature of the forecasted event. Today, such information could be effectively transmitted through the Schapi<sup>4</sup>, a flood forecasting centre that has been recently established following the devastating series of flash floods during the last decade. Together with the Observatoire Hydro-Météorologique Cévennes-Vivarais (OHM-CV) which has now established a high-density measuring network, the performance of such a forecasting system could be greatly improved with better initial conditions, calibrated hydrological model and more realistic thresholds. The radar network could then be used for confirmation of the event and more precise developments. The results show, however, that the principle can also be useful for those areas where no data are available and where the approach could greatly contribute to the preparedness for flash flood events, specifically in terms of awareness, identification of regions at risk, and potential magnitude and timing of the event.

## **Acknowledgements**

This work was carried out in the framework of the FLOODsite project funded by the FP6 Program of the European Commission under the no GOCE-CT-2004-505420. The authors would like to thank the OHM-CV for providing the radar observations and the discharge data, the Deutscher Wetterdienst for the high-resolution weather forecasting data and the DG JRC AgriFish unit for providing their meteorological data for research purposes. Also thanks should be expressed to Sandrine Anquetin from Laboratoire d'Etude des Transferts en Hydrologie et Environnement, Grenoble Université, France, and Katalin Bódis for preparing some GIS maps, as well as all colleagues from the FLOODS action that contributed with discussions to this project.

---

<sup>4</sup> Service Central d'Hydrométéorologie et d'Appui à la Prévision des Inondations.

## References

- Anquetin S., J.D. Creutin, G. Delrieu, V. Ducrocq, E. Gaume, and L. Ruin (2004) Increasing the forecasting lead-time of Weather driven flash-floods, Report on [http://natural-hazards.jrc.it/downloads/public/2004report\\_FeasibilityStudyOnFlash floods.pdf](http://natural-hazards.jrc.it/downloads/public/2004report_FeasibilityStudyOnFlash%20floods.pdf)
- Anquetin, S., Yates, E., Ducrocq, V., Samouillan, S., Chancibault, K., Gozzini, B., Pasi, F., Pasqui, M., Garcia, M., Martorell, M., Romero, R., Silvio, D., Accadia, C., Casaidi, M., Mariani, S., Ficca, G., Chesa, P., 2005, The 8 and 9 september 2002 flash-flood event in France: an intercomparison of operational and research meteorological models, *Natural Hazards and Earth System Sciences*, 5, 741-754.
- Ambroise, B., 1999: La dynamique du cycle de l'eau dans un bassin versant : processus, facteurs et modèles. Editions \*H\*G\*A\*, Bucarest, 200 pp.
- Astori, A., 1993. Morfologie alluvionali e dinamica fluviale di un fiume-torrente Alpino: il F. Tagliamento a Tolmezzo (Carnia), Master Theses, University of Padova, in Italian.
- Basara, J. B., 2001: Soil Moisture Observations for Flash Flood Research and Prediction. In: E. Grunfest and J. Handmer, eds., *Coping with flash floods*, Kluwer Academic Publishers, Dordrecht, 231-241.
- Berne, A., G. Delrieu, J. D. Creutin, and C. Obled, 2004: Temporal and spatial resolution of rainfall measurements required for urban hydrology. *Journal of Hydrology*, 5,2, 296-310.
- Borga, M., et al., 2007: Hydrometeorological Analysis of the 29 August 2003 Flash Flood in the Eastern Italian Alps. *Journal of Hydrometeorology* 8 (5), pp. 1049 – 1067.
- Borga, M., Dalla Fontana, G., Cazorzi, F., 2002: Analysis of topographic and climatic control on rainfall-triggered shallow landsliding using a quasi-dynamic wetness index. *Journal of Hydrology* 268 (1-4), pp. 56-71.
- Boudevillain, B., G. Delrieu, B. Chapon, P.-E. Kirstetter, J. Nicol and H. Andrieu, 2006, The Bollène-2002 experiment: innovative algorithms and evaluation of processing strategies for radar QPE in the Cévennes – Vivarais region, *Proceeding of the 4th European Conference on Radar in Meteorology and Hydrology*, Barcelona, 157-160.
- Brilly, M. et al., 2000: Application of meteorological mesoscale model ALADIN-SI for hydrological forecast. In: Ramirez J. A. (ED.), *Proceedings of the 20<sup>th</sup> Annual AGU Hydrology Days*. Colorado State University, Fort Collins, pp. 8 – 20.
- Casty, C., H. Wanner, J. Luterbach, J. Esper, and R. Böhm, 2005: Temperature and precipitation variability in the European Alps since 1500. *Int. J. Climatol.*, 25, 1855–1880.
- Ceschia, M., S. Micheletti, and R. Carniel, 1991: Rainfall over Friuli Venezia Giulia: High amounts and strong geographical gradients. *Theor. Appl. Climatol.*, 43, 175–180.
- Chancibault, K., S. Anquetin, V. Ducrocq and G.-M. Saulnier, 2006: Hydrological evaluation of high-resolution precipitation forecast of the Gard flash-flood event (8-9 September 2002), *Q. J. R. Meteorol. Soc.*, 132, pp 1091-1117.
- Chapon, B., 2006, Etude des pluies intenses dans la région Cévennes-Vivarais à l'aide du radar météorologique. Régionalisation des traitements radar et analyse granulométrique des pluies au sol, PhD Thesis (in French) University Joseph Fourier, Grenoble, 197 p.



Chow, V.T., Maidment, D.R. & Mays, L.M. (1988), Applied Hydrology. McGraw-Hill, Singapore.

Collier, C., 2007, Flash Flood Forecasting : What are the limits of predictability ? Q.J.R.M.S., 133, 622A, 3-23.

Colombo A.G., J. Hervàs and A.L. Vetere Arellano, 2002, Guidelines on Flash Flood prevention and mitigation. European Commission, NEDIES project.

Creutin, J.-D., Borga, M., 2003: Radar hydrology modifies the monitoring of flash-flood hazard, Hydrological Processes 17 (7), pp. 1453-1456.

Cucchi, F., et al., 2000. Studies for the realization of the hydrogeological map of Friuli – Venezia Giulia. Ipogea, 3, 57-71.

Delrieu G., V. Ducrocq, E. Gaume, J. Nicol, O. Payrastre, E. Yates, P.E. Kirstetter, H. Andrieu, P.-A. Ayrat, C. Bouvier, J.-D. Creutin, M. Livet, S. Anquetin, M. Lang, L. Neppel, C. Obled, J. Parent-du-Châtelet, G.-M. Saulnier, A. Walpersdorf and W. Wobrock<sup>1</sup>, 2005, The catastrophic flash-flood event of 8-9 September 2002 in the Gard region, France: a first case study for the Cévennes-Vivarais Mediterranean Hydro-meteorological Observatory, J. Hydrometeorology, 6, 34-52.

De Roo A., Odijk M., Schmuck G., Koster E.; Lucieer A., 2001. Assessing the effects of land use changes on floods in the meuse and oder catchment. Physics and Chemistry of the Earth, Part B: Hydrology, Oceans and Atmosphere, Volume 26, Number 7, 2001 , pp. 593-599(7)

Ducrocq V., G. Aullo and P. Santurette, 2003, Les précipitations intenses des 12 et 13 novembre 1999 sur le sud de la France. La Météorologie, 42, 18-27.

Everhardus, Christian, Ad de Roo, Steven de Jong (2002), Validation of the LISFLOOD runoff model for a mountainous catchment. Report of the European Commission, Joint Research Centre, EUR 20514 EN.

Feyen L., (2005) Calibration of the LISFLOOD model for Europe: current status and way forward, European Commission EUR22125 EN

Feyen, L., Vrugt, J.A., Ó Nualláin, B., van der Knijff, J., de Roo, A.: Parameter optimisation and uncertainty assessment for large-scale streamflow simulation with the LISFLOOD model. Journal of Hydrology (332), Issues 3-4, 276-289, 2007.12.19.

Fritsch J.M. and R. A. J. Houze and R. Adler and H. Bluestein and L. Bosart and J. Brown and F. Carr and C. Davis and R. H. Johnson and N. Junker and Y. H. Kuo and S. Rutledge and J. Smith and Z. Toth and J. W. Wilson and E. Zipser and D. Zrníc, 1998, Quantitative precipitation forecasting: report of the 8th prospectus development team, U.S. Weather Research Program, Bull. Amer. Meteorol. Soc., 79, 285-299.

Gruntfest E. and J. Handmer, 1999, Coping with Flash-Flood, Ed. NATO Science Series, 322p.

Huet P., X. Martin, J.-L. Prime, P. Foin, C. Laurain and P. Cannard, 2003, Retour d'expérience des crues de septembre 2002 dans les départements du Gard, de l'Hérault, du Vaucluse, des Bouches-du-Rhône, de l'Ardèche et de la Drôme. Technical report, Ministère de l'Ecologie et du Développement Durable, République Française, 133pp.

- KOBOLD M. and M. BRILLY, Low flow discharge analysis in Slovenia, 1994. FRIEND: Flow Regimes from International Experimental and Network Data (Proceedings of the Braunschweig Conference, October 1993). IAHS Publ. no. 221, 1994.
- Lindström, G., Johansson, B., Persson, M., Gardelin, M. & Bergström, S. (1997), Development and test of the distributed HBV-96 hydrological model. *Journal of Hydrology* 201, 272-288.
- Martinis, B., 1993. *Storia geologica del Friul*, La Nuova Base Ed., Udine.
- Mikos, M. et al, 2004. Hydrologic conditions responsible for triggering the Stože landslide, Slovenia. *Engineering Geology* 73 (2004), p. 193 – 213.
- Nuissier, O., V. Ducrocq, D. Ricard, T. Thouvenain and S. Anquetin, 2007, A numerical study of three catastrophic precipitating events over western Mediterranean region (Southern France). Part I: Numerical framework and synoptic ingredients. *Q. J. R. Meteorol. Soc.* (in press)
- Querini, R., 1977: L'influenza del terremoto sulla torrenzialità nei bacini montani del Friuli (in Italian). *Annali dell'Accademia Italiana di Scienze Forestali*, 26, 139–185.
- Ramos M.-H., Bartholmes J., Thielen-del Pozo, J. 2007 Development of decision support products based on ensemble forecasts in the European flood alert system. *Atmospheric Science Letters* 8: 113-119.
- Ruin I., J.-D. Creutin, S. Anquetin and C. Lutoff, 2007, Human exposure to flash-floods – relation between flood parameters and human vulnerability during a storm of September 2002 in Southern France, *J. of Hydrology* (submitted).
- Sénési, S., P. Bougeault, J.L. Chèze and P. Cosentino, 1996, The Vaison le Romaine Flash flood: Meso-Scale Analysis and Predictability Issues. *Wea. Forecasting*, 11, 417-442.
- Thielen J., Bartholmes J., Ramos M.-H. and de Roo., A., 2007: The European Flood Alert System, Concept and Development, Part I, HESS, 2007
- Todini E., The ARNO rainfall–runoff model, *Journal of Hydrology* 175 (1996), pp. 339–382.
- Tropeano, D., L. Turconi, and S. Sanna, 2004: Debris flows triggered by the 29 August 2003 cloudburst in Val Canale, eastern Italian Alps. *Proc. Int. Symp. INTERPRAEVENT 2004*, Riva del Garda, Italy, 121–132.
- van der Knijff, J.M., Younis, J., de Roo, A. P. J., 2008: LISFLOOD: a GIS-based distributed model for river basin scale water balance and flood simulation. *Int. J. Geographical Information Science*, accepted.
- van der Knijff J.M. and A. de Roo (2008), LISFLOOD Distributed Water Balance and Flood Simulation Model. Revised User Manual. Report of the European Commission, Joint Research Centre, EUR 22166 EN/2.
- Villi, V., G. Caleffa, G. Gatto, and G. Mori, 1986: Distribuzione spazio temporale delle piogge intense nel Triveneto- cartografia (in Italian). *Quaderno di Ricerca*, 7, C.N.R and Regione Veneto, 1–444.
- Ward, J. V., et al., 1999. A reference system for the Alps: the 'Fiume Tagliamento'. *Reg. Riv.*, 15: 63-75.
- Wood, E. F., M. Sivapalan, and K. Beven, 1990: Similarity and scale in catchment storm response. *Rev. Geophys.*, 28, 1–18.

Yates, E., J.-D. Creutin, S. Anquetin and J. Rivoirard, 2007, A scale dependant quality index of areal rainfall prediction, *J. Hydrometeorology*, 8(2): 160-170.

Younis, J., Anquetin, S., Thielen, J., 2008: The benefit of high-resolution operational weather forecasts for flash flood warning. *Hydrology and Earth System Sciences* 12 (4), pp. 1039-1051

Zhao, R. J. & Liu X. R. (1995) The Xinanjiang model. In: *Computer Models of Watershed Hydrology* (ed. by V. P. Singh), 215–232. Water Resources Publications, Colorado, USA.

European Commission

**EUR 23637 EN – Joint Research Centre – Institute for Environment and Sustainability**

**Title: Early Flash Flood Warning:**

A feasibility study with a distributed hydrological model and threshold exceedance

Author(s): Jalal Younis, Jutta Thielen

Luxembourg: Office for Official Publications of the European Communities

2008 – 55 pp. – 21 x 27.9 cm

EUR – Scientific and Technical Research series – ISSN 1018-5593

ISBN: 978-92-79-09689-1

DOI: 10.2788/38120

## **Abstract**

In Mediterranean Europe, flash flooding is one of the most devastating hazards in terms of loss of human life and infrastructures. Over the last two decades, flash floods have caused damage costing a billion Euros in France alone. One of the problems of flash floods is that warning times are very short, leaving typically only a few hours for civil protection services to act. This study investigates if operationally available short-range numerical weather forecasts together with a rainfall-runoff model can be used for early indication of the occurrence of flash floods.

One of the challenges in flash flood forecasting is that the watersheds are typically small, and good observational networks of both rainfall and discharge are rare. Therefore, hydrological models are difficult to calibrate and the simulated river discharges cannot always be compared with ground measurements. The lack of observations in most flash flood prone basins, therefore, necessitates the development of a method where the excess of the simulated discharge above a critical threshold can provide the forecaster with an indication of potential flood hazard in the area, with lead times of the order of weather forecasts.

This report is focused on four case studies in Mediterranean part of Europe: i) The September 2002-flash flood event in the Cévennes-Vivarais region in the Southeast of the Massif Central in France, a region known for devastating flash flood; ii) the August 2003-flash flood event in both Fella subcatchment of Tagliamento watershed and upstream part of Isonzo river basin, iii) the October 2006-flash flood event in Isonzo river basin and iv) the September 2007-flash flood event in Upper Sava river basin in Slovenia. The French case study is described in more detail with the principles and methodologies being explained that are then applied to the remaining three case studies. Also, there were more data available for the 1st case study.

The critical aspects of using numerical weather forecasting for flash flood forecasting are being described together with the threshold – exceedance approach previously postulated for the European Flood Alert System (EFAS). The short-range weather forecasts, from the Local model of the German national weather service, are driving the LISFLOOD model, a hybrid between conceptual and physically based rainfall-runoff model. Results of the study indicate that high resolution operational weather forecasting combined with a rainfall-runoff model could be useful to determine flash floods more than 24 hours in advance.

### **How to obtain EU publications**

Our priced publications are available from EU Bookshop (<http://bookshop.europa.eu>), where you can place an order with the sales agent of your choice.

The Publications Office has a worldwide network of sales agents. You can obtain their contact details by sending a fax to (352) 29 29-42758.





The mission of the JRC is to provide customer-driven scientific and technical support for the conception, development, implementation and monitoring of EU policies. As a service of the European Commission, the JRC functions as a reference centre of science and technology for the Union. Close to the policy-making process, it serves the common interest of the Member States, while being independent of special interests, whether private or national.



LB-NA-23637-EN-C



Publications Office  
*Publications.eu.int*

ISBN 978-92-79-09689-1



9 789279 096891